JOURNAL OF GEOPHYSICAL RESEARCH, VOL. 104, NO. B7, PAGES 15,365–15,390, JULY 10, 1999

Tectonic evolution of the Tancheng-Lujiang (Tan-Lu) fault via Middle Triassic to Early Cenozoic paleomagnetic data

Stuart A. Gilder,[1] P. Hervé Leloup,[2] Vincent Courtillot,[1] Yan Chen,[3] Robert S. Coe,[4] Xixi Zhao,[4] Wenjiao Xiao,[5] Nadir Halim,[1] Jean-Pascal Cogné,[1] and Rixiang Zhu[6]

Abstract. The north-striking Tancheng-Lujiang (Tan-Lu) fault is a conspicuous and controversial feature of the eastern Asian landscape. Near the southeast extremity of the fault in Anhui Province, we collected paleomagnetic samples at 17 Middle Triassic (T2) and 10 Upper Cretaceous (K2) to lower Cenozoic (E1) sites. T2 remanent magnetizations are interpreted as primary in two of three areas. The three areas are rotated 37° to 137° counterclockwise with respect to the South China Block (SCB) reference direction. K2-E1 remanent magnetization directions pass regional fold and reversals tests and are not rotated with respect to surrounding areas. Counterclockwise rotation of T2 strata therefore ended before K2 and is attributed to left lateral shear acting along Tan-Lu during the North China Block (NCB)-SCB collision. In Shandong Province, 700 km north of the Anhui sites, four areas containing 33 Upper Jurassic (J3) and Cretaceous sites have negligible declination differences, except for one which has dispersed directions. The fold test is inconclusive for this latter area and positive for the other three. Regional concordance of the J3-E1 paleomagnetic data (including paleolatitudes) together with observed deformation patterns suggest that an extensional regime prevailed in the Late Cretaceous and Cenozoic. Euler pole positions that constrain the North-South China collision and account for Tan-Lu motion suggest at least 500 km of sinistral shear took place along the fault, and either (1) subduction and related ultrahigh pressure (UHP) metamorphism occurred near the present location of the Qinling-Dabieshan and Sulu UHP belts while Tan-Lu acted as a transform fault that connected the two subduction zones, or (2) Tan-Lu and Sulu were parts of the same transform fault system and no UHP rocks formed in situ at Sulu. In either case, UHP rocks originally exhumed near Dabieshan could have been transported by plate capture toward Sulu along Tan-Lu. After North and South China impacted near Dabieshan, the Tan-Lu fault grew within the SCB as the Dabieshan corner indented the SCB, causing folds in SCB cover rocks to conform to the NCB margin. Late Cretaceous to Cenozoic reactivation of Tan-Lu, with both right lateral strike-slip and normal fault motion, occurred as the SCB extruded east relative to the NCB under the influence of the India-Asia collision.

1. Introduction

1.1. The General Problem

This work attempts to document the amount, sense and time of motion along a postulated major strike-slip fault that could be related to multiple tectonic episodes. Today it exhibits right lateral motion within an overall extensional environment. The question is whether this fault system was also tectonically active, and in what manner, in the early to middle Mesozoic, the Cretaceous, or the early to middle Cenozoic. Several ages and tectonic models have been proposed.

Stratigraphic sections or distinct lithologic units that crop out on opposite sides of faults are commonly used to quantify the amount and sense of offset. Indeed these arguments play a role in what is written below. However, the scientific objectiveness of this procedure must be questioned, for basins located several hundreds of kilometers apart could form in a similar tectonic environment and contain similar stratigraphies. Finally, we note that Earth scientists employ different conventions when defining collision. Here collision refers to the convergence of two continental plates since they were in contact. Collision is complete when there is no relative motion between the two plates (e.g., the India-Asia collision is not complete). With these caveats noted, we now describe an enigmatic fault located in eastern Asia.

1.2. Regional Geology and Previous Work

China contains two major tectonic blocks, the North China Block (NCB) and the South China Block (SCB),

[1]Institut de Physique du Globe de Paris, Laboratoire de Paléomagnétisme et Géodynamique, Paris, France.
[2]Institut de Physique du Globe de Paris, Laboratoire de Tectonique, Paris, France.
[3]Département des Sciences de la Terre, Université d'Orléans, Orléans, France.
[4]Earth Science Department, University of California, Santa Cruz.
[5]Laboratory of Lithosphere Tectonic Evolution, Institute of Geology, Chinese Academy of Sciences, Beijing.
[6]Institute of Geophysics, Chinese Academy of Sciences, Beijing.

Paper number 1999JB900123.
0148-0227/99/1999JB900123$09.00

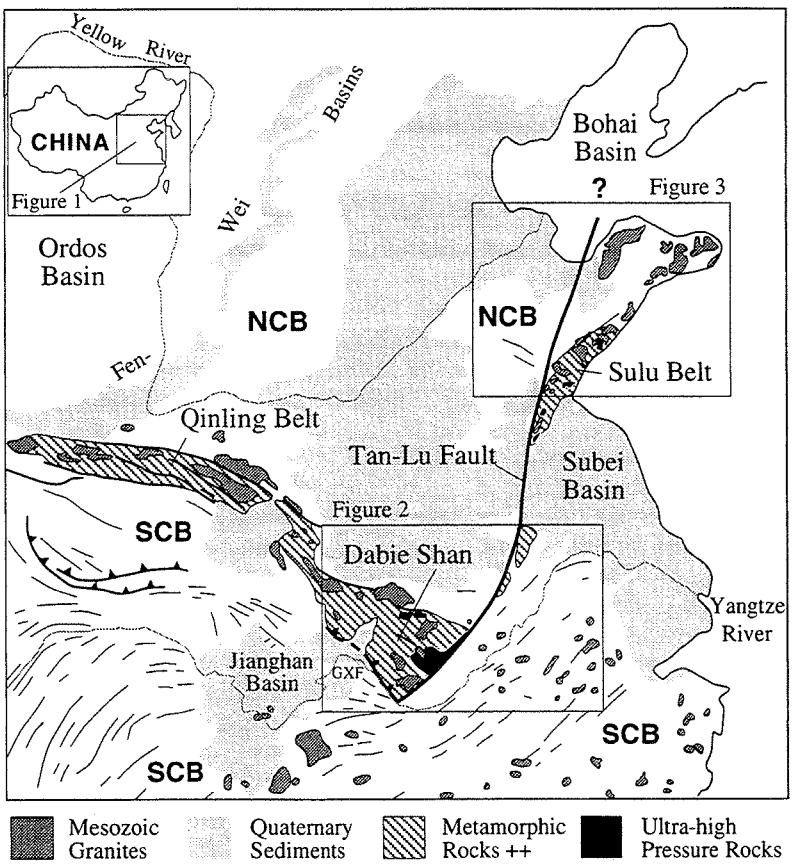

Figure 1. General geologic map of eastern China showing the Qinling and Sulu belts and the Tancheng-Lujiang (Tan-Lu) fault. Data are taken mostly from the *Academia Sinica* [1976]. GXF is the Guangji-Xiangfan fault. Note that (1) fold axes bend around Dabieshan, (2) there exists a long, narrow band of late Mesozoic granites within the Qinling-Dabieshan belt, and (3) most large Cenozoic to Quaternary basins, such as the Yellow Sea, lie north of the Qinling suture.

that are separated by the east-trending Qinling-Dabieshan suture zone (Figure 1). The Qinling-Dabieshan zone contains ophiolites, high-pressure, coesite- and diamond-bearing eclogites and has a complex history of arc accretion [e.g., *Zhang et al.*, 1984; *Wang et al.*, 1989; *Xu et al.*, 1992a, b; *Kröner et al.*, 1993]. Tectonic reconstructions of the SCB and NCB collision based on paleomagnetic data suggest that the two blocks first collided in the Permian near their eastern parts, then they progressively scissored together as the SCB rotated clockwise with respect to the NCB [*Zhao and Coe*, 1987, 1989; *Enkin et al.*, 1992]. U-Pb and Ar-Ar dates of the ultrahigh pressure (UHP) metamorphic rocks in the suture range from 245 to 170 Ma [e.g., *Reischmann et al.*, 1990; *Mattauer et al.*, 1991; *Ames et al.*, 1993, 1996; *Li et al.*, 1993; *Okay et al.*, 1993; *Eide et al.*, 1994; *Hacker and Wang*, 1995; *Hacker et al.*, 1995, 1998]. The end of collision at 159±10 Ma, near the Middle to Late Jurassic boundary, is characterized by a regional angular unconformity, a change from suture-normal shortening to suture-parallel extension, concordance of the paleomagnetic poles from both plates, and a cusp on the NCB apparent polar wander path (APWP) [*Gilder and Courtillot*, 1997]. Also found along the suture zone are a suite of granites and gneisses that yield U-Pb and Ar-Ar dates ranging from 140 to 115 Ma with the majority between 135 and 125 Ma [*Reischmann et al.*, 1990; *Li et al.*, 1993; *Eide et al.*, 1994; *Hacker and Wang*, 1995; *Ames et al.*, 1996; *Xue et al.*, 1997; *Hacker et al.*, 1995, 1998]. *Hacker et al.* [1995] proposed that the emplacement of these Lower Cretaceous granites was related to transtension along the Pacific continental margin.

The eastern part of the Qinling-Dabieshan belt is truncated by the north-striking Tancheng-Lujiang (Tan-Lu) fault. About 600 km north of the Qinling-Dabieshan belt, east of the Tan-Lu fault, a northeast-trending, coesite-bearing high-pressure metamorphic complex crops out in northern Jiangsu and southern Shandong provinces (Sulu belt) [*Hirajima et al.*, 1990; *Enami and Zang*, 1990]. U-Pb and Ar-Ar dates of the UHP mineral assemblages range from 217 to 194 Ma [*Chen et al.*, 1992; *Ames et al.*, 1996]. Similarities of metamorphic mineral assemblages and their ages could suggest both eclogite-bearing complexes were once part of the same belt that was later displaced by sinistral shear along the Tan-Lu fault [e.g., *Xu et al.*, 1987]. These similarities are further corroborated by oxygen isotope compositions which are among the most negative of any metamorphic rock [*Yui et al.*, 1995, 1997; *Zhang et al.*, 1998]. Like the

Qinling-Dabieshan suture, the Sulu belt contains Lower Cretaceous granites whose Ar-Ar dates range from 123 to 115 Ma [*Chen et al.*, 1992].

The Tan-Lu fault system is easily identifiable on geologic maps because rock types change abruptly across it (Figures 1 to 3). Paleozoic stratigraphic sequences typical of the SCB are found east of the Tan-Lu fault and south of Sulu, whereas they are typical of the NCB west of Tan-Lu [e.g., *Zhang et al.*, 1984]. In Anhui Province (Figure 2), Tan-Lu is mapped as a normal fault separating Dabieshan to the west from Upper Cretaceous to Early Cenozoic continental sediments of the Qianshan basin to the east. Northeast of Hefei (Figure 2), the fault zone is more diffuse. Upper Cretaceous redbeds and Late Jurassic volcanics are in normal fault contact with Proterozoic rocks. We note that these Proterozoic rocks could potentially contain UHP Dabieshan-like lithologies. Farther north in Shandong Province (Figure 3), the Tan-Lu fault zone divides abundant Paleozoic sediments, no Mesozoic granites, and no UHP metamorphic rocks on the west from no Paleozoic sediments, abundant Mesozoic granites and UHP metamorphic rocks on the east. The fault zone in Shandong is mapped as four major normal faults that form two grabens, filled with Cretaceous continental sediments, separated by a horst comprised mostly of Archean basement and Paleozoic sediments. In the region spanning from Shandong to Anhui, regional magnetic fields on both sides of Tan-Lu are different, and the fault zone forms a linear anomaly in between [*Wei and Teng*, 1993]. *Wei and Teng* [1993] attribute the magnetic signature to differences in upper crustal composition, with Tan-Lu acting as a deep-seated fault zone dividing two distinct massifs. Earthquake focal mechanisms, heat flow, and sedimentation within the Bohai Basin (Figure 1) suggest that this region is presently evolving as a series of pull apart basins along north-northeast-striking right lateral faults within an extensional environment [e.g., *Ye et al.*, 1985; *Chen and Nábelek*, 1988].

Because the southern part of the Tan-Lu fault terminates at the SCB (Figure 1), it is inferred that lateral motion along Tan-Lu ceased when the two blocks sutured together. However, this constraint is not universally accepted [e.g., *Xu et al.*, 1987; *Kimura et al.*, 1990]. Although the geologic details of the UHP terranes are beyond the scope of this paper, the location of the suture and southern limit of Tan-Lu requires some discussion. Most $^{147}Sm/^{144}Nd$ ratios and depleted mantle model ages of Dabieshan granites have SCB affinities [*Chen and Jahn*, 1998]. Thus the original subduction zone should lie somewhere north of Dabieshan (see also *Hacker et al.* [1998]). However, during active collision, the locus of subduction may jump into the subducting plate as new major intracontinental thrust faults are initiated. Material from the subducting plate is transferred to the overriding plate in the process. Such material, which had undergone UHP metamorphism, would have geochemical affinities with the subducting plate and may be exhumed as collision continues [e.g., *Chemenda et al.*, 1995, 1996]. This has two important implications for Dabieshan: (1) exhumation of the UHP rocks probably occurred continuously during collision as evidenced by a >50 million year spread in U-Pb and Ar-Ar dates, and (2) although the original suture was likely north of Dabieshan, the final locus of subduction was probably along the Guangji-Xiangfan fault, which is the southern limit of the exposed UHP rocks (Figures 1 and 2) [e.g., *Xue et al.*, 1996]. Thus most tectonic maps, including ours, extend Tan-Lu to the Guangji-Xiangfan fault.

Several tectonic models of the Tan-Lu fault have been put forth and suggestions for the age of large-scale displacement along the fault range from Precambrian to Cenozoic (see review by *Xu* [1993]). More recent models fall into two categories: syn- and post-NCB-SCB collision. Of the syncollisional scenarios, *Yin and Nie* [1993] published an indentation model of the collision. According to their model, the southern border of the NCB was a long-lived Andean-type margin contiguous across the Qinling and Sulu metamorphic belts. They proposed that the northeast part of the SCB protruded approximately 600 km farther north than the rest of the block. Thus the collision began in the east where the SCB extended northward, and the Tan-Lu fault grew as the buttress progressively indented the eastern part of the NCB.

Li [1994] presented a crustal detachment model based on the interpretation of aeromagnetic anomalies. Similar to the *Yin and Nie* [1993] model, *Li* [1994] proposed that an Andean-type margin extended eastward from Qinling to Sulu. During the NCB-SCB collision, the NCB indented the SCB and displaced the suture in a sinistral sense along a 115 km translithospheric fault. As the collision continued, east of Tan-Lu, the upper crust of the SCB detached from the lower crust and was thrust >400 km over the NCB in a thin-skin tectonics style, increasing the apparent offset to >515 km.

Postcollision tectonic models are segregated into two camps. The first believes Tan-Lu was a part of a 4000-km-long transform fault system that spans from South China to the Bay of Okhotsk [e.g., *Xu et al.*, 1987; *Yanai et al.*, 1993]. Supporting the notion that large-scale sinistral motion occurred along the fault north of Sulu, *Chen* [1993] described peculiar Upper Jurassic andesite flows and similar Lower Cretaceous (Hauterivian) stratigraphic sections that crop out on either side of the Tan-Lu fault, separated by 740 km in a left-lateral sense. Uppermost Lower Cretaceous (Aptian-Albian) lacustrine black sandstones, mudstones, and shales found on both sides of the fault are not significantly offset [*Chen*, 1993]. Thus, if the correlations are correct, horizontal displacement on Tan-Lu occurred between the Hauterivian and the Albian spanning ~18 m.y. This timing is compatible with the mean K-Ar date (99±2 Ma) of five whole-rock mylonite samples found in a granite lying near the Tan-Lu fault zone [*Zhu et al.*, 1995, Figure 2, locality z]. To date, these thin (<1 m) mylonite ribbons represent the only direct evidence suggesting sinistral motion occurred on or near the fault. The second camp suggests the Tan-Lu fault was a major transcurrent fault that was activated as the SCB extruded to the east either due to a postulated Early Cretaceous collision of the Indochina block with Asia [*Kimura et al.*, 1990] or to the Cenozoic India-Asia collision [*Uchimura et al.*, 1996].

In light of the ambiguities, and with the intent to better understand the timing and kinematics of the Tan-Lu fault,

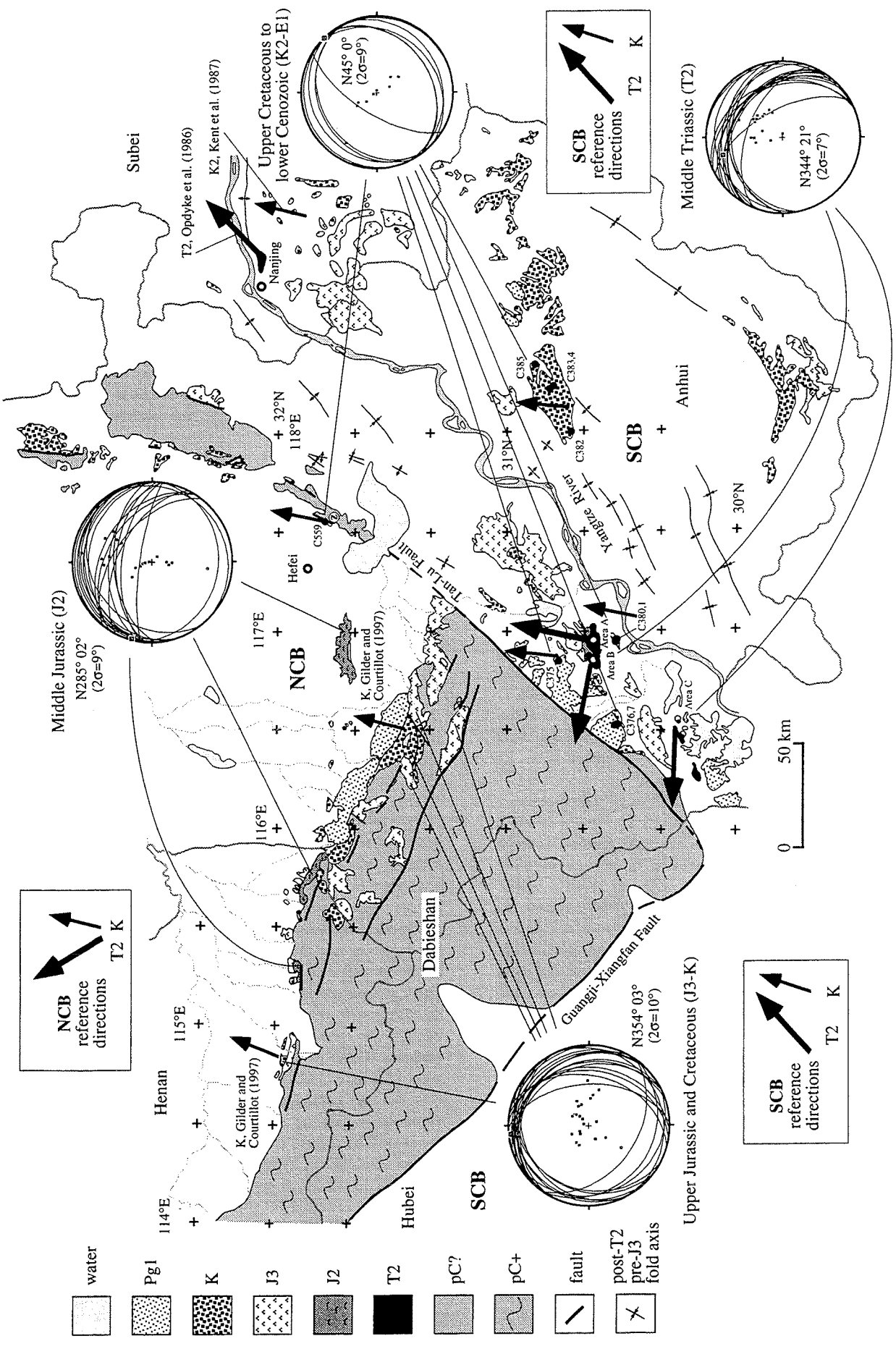
Subei
Upper Cretaceous to lower Cenozoic (K2-E1)
T2, Opdyke et al. (1986)
K2, Kent et al. (1987)
Nanjing
N45° 0°
(2σ=9°)
SCB reference directions
T2 K
Middle Triassic (T2)
N344° 21°
(2σ=7°)
Middle Jurassic (J2)
N285° 02°
(2σ=9°)
32°N
118°E
Hefei
C559
117°E
NCB
K. Gilder and Courtillot (1997)
Tan-Lu Fault
31°N
C385
C383.4
C382
SCB
Anhui
Yangtze River
30°N
Area A
Area B
Area C
C380.1
C376.7
C375
116°E
Dabieshan
Guangji-Xiangfan Fault
50 km
0
NCB reference directions
T2 K
115°E
Henan
K. Gilder and Courtillot (1997)
114°E
Hubei
SCB
N354° 03°
(2σ=10°)
Upper Jurassic and Cretaceous (J3-K)
SCB reference directions
T2 K
water
Pg1
K
J3
J2
T2
pC?
pC+
fault
post-T2 pre-J3 fold axis

we carried out a paleomagnetic study in Anhui and Shandong provinces where the Tan-Lu fault is best characterized.

2. Geology and Sampling

Collecting rocks to test the possible Tan-Lu tectonic scenarios is a difficult task because they must be of the appropriate age, exposed, accessible, solid enough to sample, reliable recorders of the ancient Earth's magnetic field, and have identifiable paleohorizontal indicators (e.g., bedding planes). In Anhui, we sampled primarily Middle Triassic (T2) and post-Lower Cretaceous (K1) rocks because the rocks of these ages meet these criteria. We only found one Upper Jurassic (J3) and one Middle Jurassic (J2) site whose bedding was visible and whose lithology was suitable for a paleomagnetic study, unlike most of the coarse conglomerates, breccias, and volcanic rocks of these ages we encountered. Thus J3 and J2 rocks are not reported in this study from Anhui. To our knowledge, no pre-J3 sediments crop out in Shandong Province east of Tan-Lu, and thus no pre-J3 rocks were collected there. Understanding the structural geology is also important not only to apply the proper fold test correction but also to help decipher the deformation history of the area. During sampling we questioned whether the same change in fold patterns occurred east of Tan-Lu as were observed west of Tan-Lu in an earlier study [*Gilder and Courtillot*, 1997].

2.1. Anhui Province

Field missions in 1993 and 1995 netted 219 samples from 27 sites east of the Tan-Lu fault in Anhui Province (Figure 2). Eleven sites of T2 Tongtoujian Formation purple siltstones were sampled near the town of Yueshan. Nine sites come from places near roads or foot paths that access the Anqing copper mine, nearby reservoir and Ma'an village (30.64°N, 116.93°E, sites C379, C541-4, C548-50, and C558) (area A, Table 1). The beds at these sites dip northeast. Near Cha village (30.64°N, 116.83°E), about 10 km west of Yueshan, lies the Lingerchong reservoir where we sampled two more T2 Tongtoujian Formation sites (C545-6) (area B, Table 1). The rocks near this reservoir are more intensely folded than those nearer to Yueshan; Lower Jurassic (J1) sediments we saw there were convoluted. The T2 age of the Tongtoujian Formation is well constrained by 17 species of bivalves, plant fossils (*Annalepis zeilleri* Frich) and charophytes (*Stellatochara*) [*Anhui Bureau of Geology and Mineral Resources* (AHBGMR), 1987, p. 145]. At Yueshan, the formation is both under and overlain by fossil rich carbonates (Nanlinghu Formation) and coal-bearing (Lalitou Formation) strata, respectively. The Tongtoujian Formation correlates in both sedimentology and magnetization characteristics (see below) with the T2 Puxi and Badong formations in Hubei and Hunan provinces located ~800 km west-southwest of our sites [*Huang and Opdyke*, 1996, 1997].

We also sampled six Tongtoujian sites 50 km southwest of Yueshan (area C, Table 1)- two sites near Jinlong village (30.23°N, 116.47°E), off the road that connects Wangjiang and Taihu cities, and four sites to the northeast (30.25°N, 116.54°E) in a small quarry near the road connecting Wangjiang and Huaining cities. These sites are marked as Tongtoujian Formation on the provincial geologic map [*AHBGMR*, 1987]; however, they do not possess the purple color or silt-sized particles (most are red and sand-sized), nor did we observe the underlying limestone facies or overlying coal beds, characteristic of the Tongtoujian Formation that we sampled farther northeast.

Ten sites of Upper Cretaceous (K2) to early Cenozoic (E1) samples were drilled over a broad area (Figure 2). Three E1 Wanghudun Formation sites (C375 at 30.77°N, 116.82°E and C376-7 at 30.52°N, 116.5°E) in the Qianshan basin, two E1 sites (C380-1 at 30.53°N, 116.9°E) at exposures about 10 km northwest of Anda city near the bank of the Yangtze river, four uppermost Cretaceous (Xuannan Formation) sites (C382 at 30.71°N, 118.0°E, C383-4 at 30.8°N, 118.25°E and C385 at 30.83°N, 118.37°E) in the Nanling basin, and one K2 site (C559, Changqiao Formation at 31.78°N, 117.55°E) situated some hundreds of meters west of the present trace of the Tan-Lu fault. The K2 and E1 sites are comprised of red to pink, relatively coarse grained sandstones. We accepted the ages of the strata as indicated on the provincial geologic map [*AHBGMR*, 1987]. The K2 ages are largely constrained by pollens, bivalves and ostracods [*AHBGMR*, 1987, pp. 170-175], as are the E1 ages, the latter also contain vertebrate fossils [*AHBGMR*, 1987, pp. 185-186].

2.2. Shandong Province

A field mission in 1996 to Shandong Province netted 356 samples from 40 Triassic to Cretaceous sites (Figure 3, Table 2). The samples come from four general areas: (area I) Wulian (35.75°N, 119.2°E), (area II) Mengyang (35.72°N, 117.93°E), (area III) 15 km SE of Zibo (36.6°N, 117.9°E), and (area IV) Laiyang (36.98°N, 120.73°E). Sites in areas I and III were previously sampled and demagnetized by *Lin* [1984] and *Zhu* [1993] (see discussion below). The ages assigned to most of the continental sediments in Shandong have recently changed [*Liu et al.*, 1994; *Zhang et al.*, 1994]. The units around areas I and IV were generally segregated into three populations: the Upper Jurassic (J3) Laiyang Group, the

Figure 2. "opposite." Simplified geologic map of Anhui Province and eastern Henan Province [from *AHBGMR*, 1987; *HNBGMR*, 1992]. Triassic localities are shown as white circles; Late Cretaceous to early Cenozoic localities as black circles. Bedding attitudes are from this study and *Gilder and Courtillot* [1997]; bedding planes are plotted on the lower hemisphere and poles to bedding on the upper hemisphere (open squares) unless beds are overturned (J2 only, solid dots); fold axis is represented by large squares. Large and small arrows show the declination component of the Middle Triassic and the Cretaceous to early Cenozoic paleomagnetic data, respectively. The symbol z denotes the 99±2 Ma mylonite locality described by *Zhu et al.* [1995].

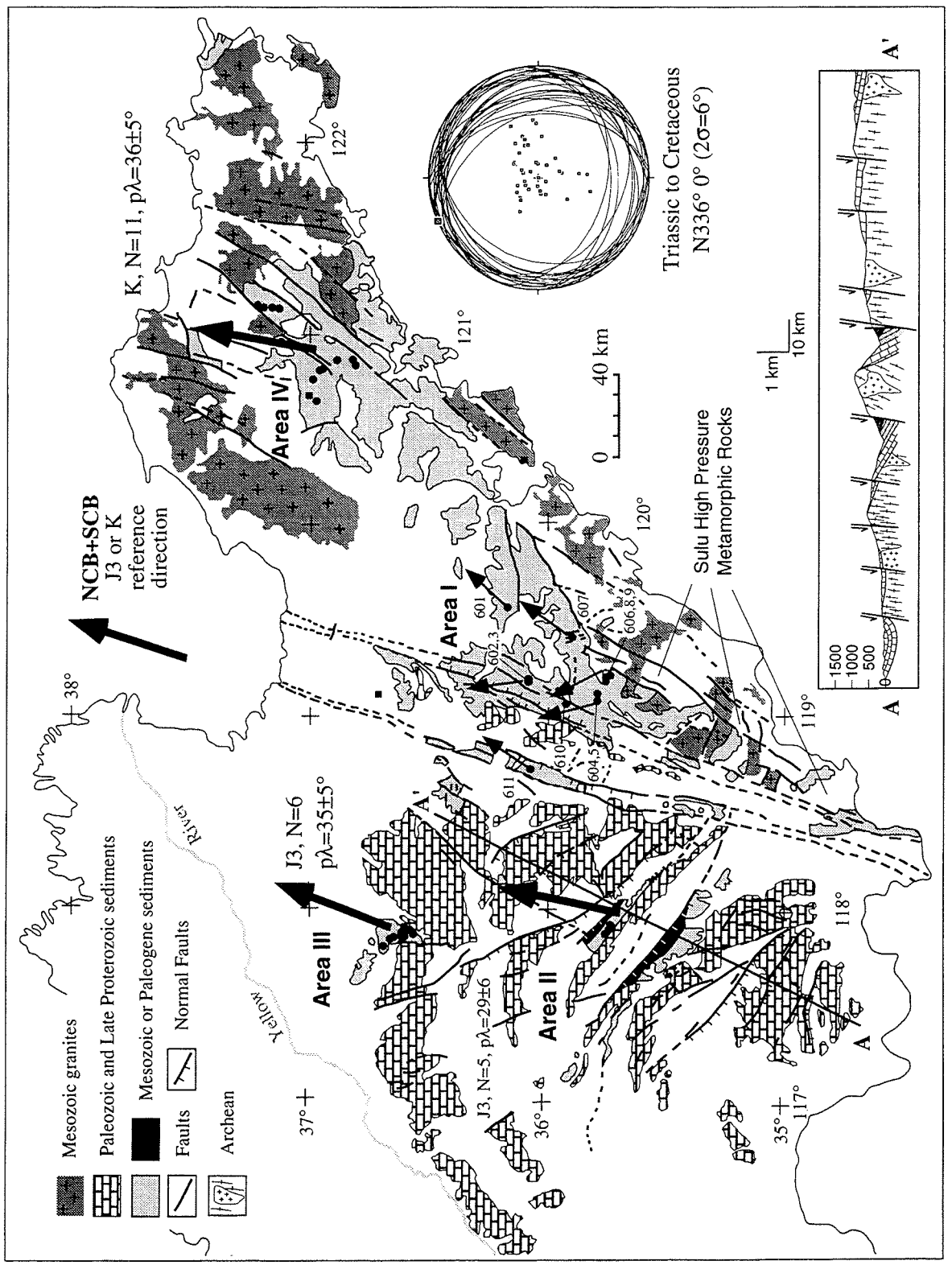

Figure 3. Simplified geologic map and cross section of Shandong Province (from *SDBGMR* [1991] and this study). Sampling localities are filled circles. Large arrows represent tilt corrected, area mean declinations. Small arrows represent tilt corrected, site mean declinations (or average of few sites from same general location). Same conventions in stereonet plot as in Figure 2. Note 10x vertical exaggeration in cross section.

Table 1. High-Temperature Component Paleomagnetic Data From Anhui Province

Site	no/No	N/R	*Dg*	*Ig*	*Ds*	*Is*	*k*	α_{95}	DD	Dip
					Middle Triassic					
Area A										
C379	13/13	0/13	356.0	81.7	17.9	30.9	45.2	6.2	22.1	51.5
C541	9/9	9/0	350.9	59.2	8.9	28.6	106.7	5.0	31.0	35.0
C542	9/9	9/0	341.8	51.3	12.8	37.5	307.1	2.9	64.2	33.0
C543	9/9	9/0	340.0	56.0	2.8	26.8	273.2	3.1	32.7	37.5
C544	6/6	6/0	336.5	58.0	9.7	40.5	206.1	4.7	52.2	32.0
C548	9/9	9/0	354.9	63.1	15.1	33.0	96.5	5.3	35.7	34.3
C549	5/5	5/0	342.5	65.7	7.0	36.6	240.3	4.9	28.7	34.0
C550	8/8	8/0	315.0	52.3	16.9	33.0	167.2	4.3	61.3	60.0
C558	9/9	9/0	355.2	65.3	20.2	34.2	36.5	8.6	41.7	36.3
Mean	9L/9L	-	341.5	61.9			52.8	7.1		
Mean	9L/9L	-			12.3	33.6	157.1	4.1		
Area B										
C545	8/8	8/0	271.3	20.5	280.6	25.0	128.5	4.9	17.3	22.3
C546	9/9	9/0	250.8	47.2	280.9	43.4	52.5	7.2	348.7	29.0
Mean	17s/17s	-	262.2	35.0			19.2	8.4		
Mean	17s/17s	-			280.8	34.7	37.9	5.9		
Area C										
C552	9/9	9/0	272.5	47.2	273.0	51.2	21.8	11.3	86.7	4.0
C553	9/9	8/1	250.7	23.5	256.4	24.0	3.8	28.9	345.7	13.0
C554	9/9	9/0	263.8	27.9	282.3	50.0	11.9	15.6	47.2	31.0
C555	6/8	6/0	288.2	29.4	306.3	48.5	40.0	10.7	67.7	28.7
C556	8/9	8/0	267.1	32.0	286.2	27.7	27.2	10.8	359.2	32.5
C557	9/9	9/0	291.3	32.4	303.9	17.5	14.8	13.8	358.7	30.0
Mean	6L/6L	-	272.0	32.9			27.4	13.0		
Mean	6L/6L	-			284.6	37.8	14.3	18.3		
					Upper Cretaceous to Lower Cenozoic					
C375	7/7	7/0	20.5	55.3	5.5	46.4	31.5	10.9	319.0	15.0
C376*	0/9								331.5	23.0
C377*	0/4								326.5	26.0
C380	6/7	0/6	0.4	32.0	15.0	44.6	27.7	13.0	132.0	22.0
C381	5/5	0/4	6.7	39.5	8.3	39.3	37.1	13.1	87.0	2.0
C382	6/8	6/0	344.1	37.9	346.4	52.7	20.1	15.3	156.3	15.0
C383	6/7	6/0	354.2	29.2	9.8	51.8	49.9	9.6	143.3	28.5
C384	8/8	8/0	0.8	31.6	19.4	52.3	41.6	8.7	145.3	28.5
C385*	0/10								336.1	4.0
C559	7/7	7/0	70.5	29.8	12.2	43.9	27.2	11.8	301.9	66.8
Mean	7L/10L	-	9.5	39.5			11.1	18.9		
Mean	7L/10L	-			8.4	47.7	90.3	6.4		

Abbreviations are no/No, number of samples used to calculate mean direction/number of samples demagnetized; N/R, normal (N) or reversed (R) polarity (note that no polarity was assigned to samples fit with great circles); *D*, declination; *I*, inclination; *g*, in situ (geographic) coordinates; *s*, tilt-corrected (stratigraphic) coordinates (at 100% unfolding); α_{95}, the radius that the mean direction lies within 95% confidence; *k*, the best estimate of the precision parameter; DD, dip direction of beds; s, samples; L, localities.

*No HTC was isolated in these sites.

Lower Cretaceous (K1) Qingshan Group and the Upper Cretaceous (K2) Wangshi Group [*Shandong Bureau of Geology and Mineral Resources* (SDBGMR), 1991, pp. 170-190]. In *SDBGMR* [1991, p. 550], it is stated that, "There is much controversy as whether the biotas in the Fengshuiling and Laiyang Formations belong to the Jurassic or the Cretaceous." The most recent analysis, based on stratigraphic correlation, suggests that most of the J3 to K2 sediments should be considered as K1 [*Liu et al.*, 1994], consistent with the available K-Ar dates of the volcanics (127 to 107 Ma [*SDBGMR*, 1991, p. 550]) which are intercalated with the sediments. Thus, most of the volcanic and continental sediments in the Shandong basins east of Tan-Lu are now classified as the K1 Laiyang Group [*Liu et al.*, 1994].

Similar changes in age assignments have been made to the continental sediments west of the Tan-Lu fault. For example, the fossil-poor Fenghuangshan Formation was assigned a Triassic age before being designated Upper Permian [*SDBGMR*, 1991, p. 548]. The most recent compilation based on stratigraphy classifies the formation as the Triassic (unspecified) Shihezi Formation [*Zhang et al.*, 1994], of which we sampled six sites in region III. Likewise, stratigraphic analyses have reclassified the red continental sediments of the Middle to Upper Jurassic Santai Formation as Upper Jurassic [*Liu et al.*, 1994]. We sampled six Santai Formation sites in area III and five in area II. The area III sites often crop out as red fossil sand dunes, making it sometimes quite difficult to identify the paleohorizontal bedding planes.

Table 2. High-Temperature Component Paleomagnetic Data From Shandong Province

Site	Age	no/No	N/R	*Dg*	*Ig*	*Ds*	*Is*	*k*	α_{95}	DD	Dip
					Area I						
C601	K1	8/8	8/0	46.5	35.2	40.1	30.2	36.9	9.2	344.0	10.0
C602	K1	9/9	9/0	349.6	35.9	345.5	64.8	25.0	10.5	174.1	29.0
C603	K1	8/8	8/0	356.5	27.1	356.6	62.4	21.3	12.3	176.3	35.3
C604	K1	11/11	9/2	15.9	59.6	342.5	45.4	35.0	7.8	297.6	28.1
C605	K1	10/10	10/0	351.0	59.4	347.5	43.8	127.0	4.3	339.4	15.8
C606	K1	11/11	0/11	327.9	35.5	335.0	39.7	31.2	8.3	85.6	10.0
C607	K1	10/10	10/0	30.1	45.4			101.7	4.8	121.7*	10.3*
C607	K1	10/10	10/0			35.3	42.7	69.3	5.8		
C608	K1	9/9	0/9	324.1	20.9	326.9	38.5	18.9	12.2	130.1	18.3
C609	K1	9/9	0/9	340.0	33.9	336.6	37.6	102.5	5.1	210.1	6.0
C610	K	9/9	9/0	352.9	53.4	266.5	76.1	355.7	2.7	195.3	39.0
C611	K1	7/8	7/0	329.9	61.7	32.6	63.9	134.0	5.2	94.8	30.0
					Area II						
C612	J3	9/9	2/1	352.8	66.2	7.8	49.4	62.5	7.0	29.6	19.0
C613	J3	9/9	1/2	346.9	68.3	8.2	51.4	178.5	4.1	33.9	20.5
C614	J3	11/11	3/5	338.4	50.9	5.5	44.2	9.1	16.1	67.1	25.0
C615	J3	8/9	8/0	7.0	63.7	16.3	44.7	18.8	13.1	30.1	20.0
C616	J3	7/8	7/0	357.8	68.0	24.2	50.4	98.5	6.1	53.1	23.0
Mean	J3	5L/5L	-	351.4	63.8			83.5	8.4		
Mean	J3	5L/5L	-			12.3	48.2	174.6	5.8		
					Area III						
C617	T	5/5	5/0	21.1	63.6	8.2	64.4	556.7	3.2	277.3	6.3
C621	T	7/7	7/0	18.8	50.6	18.8	50.6	209.3	4.2	0.0	0.0
C622	T	7/7	7/0	19.3	68.3	347.2	71.0	229.8	4.0	260.6	12.0
C623	T	9/9	9/0	336.8	51.3	331.7	41.4	296.0	3.0	308.1	11.0
C624	T	8/8	8/0	34.0	73.4	346.4	63.1	179.4	4.1	307.1	20.5
C625†	T	0/0								16.6	11.0
Mean	T	5L/5L	-	10.4	63.0			30.3	14.1		
Mean	T	5L/5L	-			353.7	59.5	25.7	15.4		
C618	J3	7/7	7/0	40.5	57.7	26.2	53.5	224.9	4.0	327.3	10.7
C619	J3	8/8	8/0	51.2	59.6	18.4	57.3	157.2	4.4	311.1	19.8
C620	J3	5/5	5/0	47.5	60.8	19.4	53.7	89.6	8.1	324.6	19.0
C626†	J3	0/0								24.6	13.0
C627	J3	5/5	5/0	302.1	68.5	11.2	61.6	107.0	7.4	56.0	30.0
C628	J3	9/9	2/3	303.7	62.7	20.1	53.1	111.8	5.1	62.3	43.0
C629	J3	7/8	0/7	345.8	59.7	24.7	44.7	44.7	9.1	69.6	32.0
Mean	J3	6L/6L	-	8.1	69.1			13.7	18.8		
Mean	J3	6L/6L	-			20.5	54.0	162.2	5.3		
					Area IV						
C630	K	8/8	8/0	4.9	35.6	10.0	51.3	29.2	10.4	168.6	16.5
C631	K	5/7	5/0	357.3	27.5	342.7	45.2	267.0	4.7	218.1	26.0
C632	K1	9/9	9/0	19.4	44.5	6.8	52.2	120.9	4.7	248.6	13.5
C633	K1	9/9	0/2	30.2	42.1	22.0	47.4	28.0	10.6	263.6	9.8
C634	K1	8/9	8/0	328.3	64.9	17.1	60.0	303.6	3.2	72.6	24.7
C635	K	7/7	7/0	346.1	58.5	4.7	57.6	148.2	5.0	81.1	11.5
C636	K1	9/9	9/0	3.0	40.9	9.7	54.8	89.9	5.5	162.7	15.2
C637	K1	8/8	8/0	310.6	50.1	17.7	60.1	671.3	2.1	84.8	42.8
C638	K1	7/8	7/0	320.4	43.2	7.9	53.8	245.4	3.9	87.6	40.2
C639	K1	8/8	8/0	327.1	64.6	21.4	57.0	178.2	4.2	71.2	29.3
C640	K1	8/8	8/0	14.8	64.1	19.4	57.2	304.9	3.2	37.9	7.0
Mean	K	11L/11L	-	353.4	51.5			15.0	12.2		
Mean	K	11L/11L	-			10.3	54.8	92.9	4.8		

See Table 1 for abbreviations. Other abbreviations are T, Triassic; J, Jurassic; K, Cretaceous; 1, Early; 3, Late.
*Mean value.
†Samples disintegrated during demagnetization.

2.3. Age of Folding

West of the Tan-Lu fault in Anhui Province, Gilder and Courtillot (1997) found that the bedding attitudes of J2 beds define fold axes trending N285°02° (2σ=9°), parallel to the Qinling-Dabie suture, whereas J3 to K tilt axes trend N354°03° (2σ=10°), perpendicular to the suture (Figure 2). Some J2 beds are overturned; J3 and younger beds rarely dip more than 30°. These folding relationships imply that (1) a regional angular unconformity separates J2 from J3 strata, as suggested by *AHBGMR* [1987, pp. 153-168], and (2) that north-south contraction ended in the upper J2 or lower J3. The gentle dips of the J3 and K beds suggest they were likely tilted in an east-west extensional environment during or after K2.

In Anhui Province, east of the Tan-Lu fault, T2 beds from our sampling sites define a fold axis trending N344° and plunging 21° (2σ=7°). This uncertainty is likely

underestimated because of the relatively small angle of convergence [*Schmidt*, 1985]. The ten K2 to E1 sites define a horizontal (0°) fold axis trending N45° (2σ=9°). The only site of the younger age group that has a dip exceeding 30° is C559, which crops out a few 100 m from the trace of the Tan-Lu fault. There the beds dip 67° to the west and are cut by several normal faults dipping about the same amount or less in the opposite direction, typical of tilted block structures formed in attenuated crust [e.g., *Morton and Black*, 1972]. These data suggest that the post-Jurassic beds were tilted in an extensional regime in the Cenozoic. Because the T2 strata strike mostly northwest and have plunging fold axes, and the K2-E1 strata strike northeast and have horizontal fold axes, a regional angular unconformity likely separates T2 from K2-E1. This is consistent with the angular unconformity described by *AHBGMR* [1987, p. 155] in nearby Nanling County where gently dipping Upper Jurassic Zhongfencun Formation sediments unconformably overlie steeply dipping Tongtoujian Formation red beds. The regional angular unconformities in both east and west Anhui likely occurred at the J2-J3 boundary, separating the time of active NCB-SCB collision below, from postcollision above. We note that the N344° trend of the T2 fold axes of our sites does not conform to the regional northeast trend of the post-T2, pre-J3 fold axes observed in southern Anhui (Figures 1 and 2). This is likely due to local tectonic effects approaching the Tan-Lu fault (see below).

The cross section west of the Tan-Lu fault in Shandong Province (Figure 3, note 10x vertical exaggeration) highlights the absence of significant folding between the Late Proterozoic and the Cretaceous. All post-Late Proterozoic sediments along this section are tilted by normal faults. The only angular unconformity lies within the middle Cenozoic; it signifies different degrees of tilting and not prior folding of the underlying beds. This compressional hiatus is also suggested by the geologic and isotopic constraints from localities within the fault zone as described by *Fletcher et al.* [1995], who found that Late Proterozoic beds are flat lying and Rb-Sr and K-Ar dates of ductily deformed gneisses are largely >1.7 Ga. For these reasons, the stereonet of the poles to bedding and bedding planes from Shandong Province in Figure 3 does not segregate the data based on age. Moreover, the fold axes east and west of Tan-Lu trend nearly the same, so all sites are plotted together in the stereonet. Dips of the 40 sites rarely exceed 30°, and the bedding attitudes define a horizontal (0°) fold axis trending N336° (2σ=6°). There is a notable resemblance between this plot and the stereonet of J3-K bedding data from the Qinling-Dabieshan belt (Figure 2). The interpretation of both plots is likely the same: tilting occurred during east-west extension in the Late Cretaceous or thereafter. Alternatively, the sediments could have filled asymmetric half grabens with extension occurring as early as J3 or K1. A slight angular unconformity between Cretaceous and middle to late Paleogene sediments is indicated on the geologic map and accompanying text published by *SDBGMR* [1991] (Figure 3, cross section), suggesting that the region has experienced a few episodes of extension. Multiple extensional events have been proposed by several workers (see review by *Gilder et al.* [1991]), however detailed kinematic analyses to understand extension direction, etc. have not been performed.

3. Paleomagnetism

Rocks were cored in the field using a portable drill. A device mounted with a magnetic compass oriented the cores. Sun compass readings were obtained during orientation to correct for local magnetic declination anomalies. The cores were cut into cylindrical samples measuring 2.5 cm in diameter and 2.2 cm in length. Samples were demagnetized in mu metal-shielded ovens over 12-24 temperature steps and subsequently measured either with a CTF two or three-axis superconducting magnetometer or a JR-5 spinner magnetometer housed in the magnetically shielded Paleomagnetic Laboratory at the Institut de Physique du Globe de Paris. Samples collected in 1993 were thermally demagnetized and measured using a 2G three-axis superconducting magnetometer housed in a magnetically shielded room at the University of California, Santa Cruz. Bulk susceptibility was measured after every demagnetization step for about three samples per site to signal whether chemical changes were affecting the magnetization during progressive heating. *Zijderveld* [1967] and stereonet plots were constructed from the demagnetization data of each sample and characteristic directions were determined using principal component analysis [*Kirschvink*, 1980]. Site and study means were calculated with *Fisher* [1953] statistics. The *Watson and Enkin* [1993] fold test was employed using 1000 simulations and assuming 5° circular standard deviations for bedding attitudes. Great circles helped define the characteristic directions for some samples in six (of 65) sites using the *McFadden and McElhinny* [1988] method. The description of the magnetizations given below are in in situ coordinates unless otherwise specified.

3.1. Anhui Province

3.1.1. Middle Triassic. The vast majority of the 147 T2 samples from 17 sites at all three areas yielded well-defined characteristic components (Table 1, Figures 4 and 5). After cleaning away a viscous component in the first few demagnetization steps, most samples contained two north to west and down oriented components. In most cases, low-temperature components (LTC) (<640°C) did not decay to the origin, whereas high-temperature components (HTC) (>640°C) did. Best-fit line segments were applied relatively systematically to the same temperature steps at each site. Because the HTC directions differ at the three geographical areas, they are discussed separately. In all cases, low field susceptibility versus temperature determinations, unblocking temperatures of 680°-700°C and the purple or red color of the samples suggest the magnetic remanence is carried by hematite. Demagnetization characteristics such as the isolation of two components and their separation around 640°C is very similar to that found by *Huang and Opdyke* [1996, 1997] for T2 red beds in Hubei and Hunan provinces.

Most samples from area A had two north to northwest and down directed magnetic components (Figures 4a to 4d). Samples from site C379 possessed solely reversed polarity directions after removal of a north and down directed LTC (Figures 4e and 4f). For the eight sites with two normal polarity components, the HTC was often distinguished from the LTC by shallower inclinations.

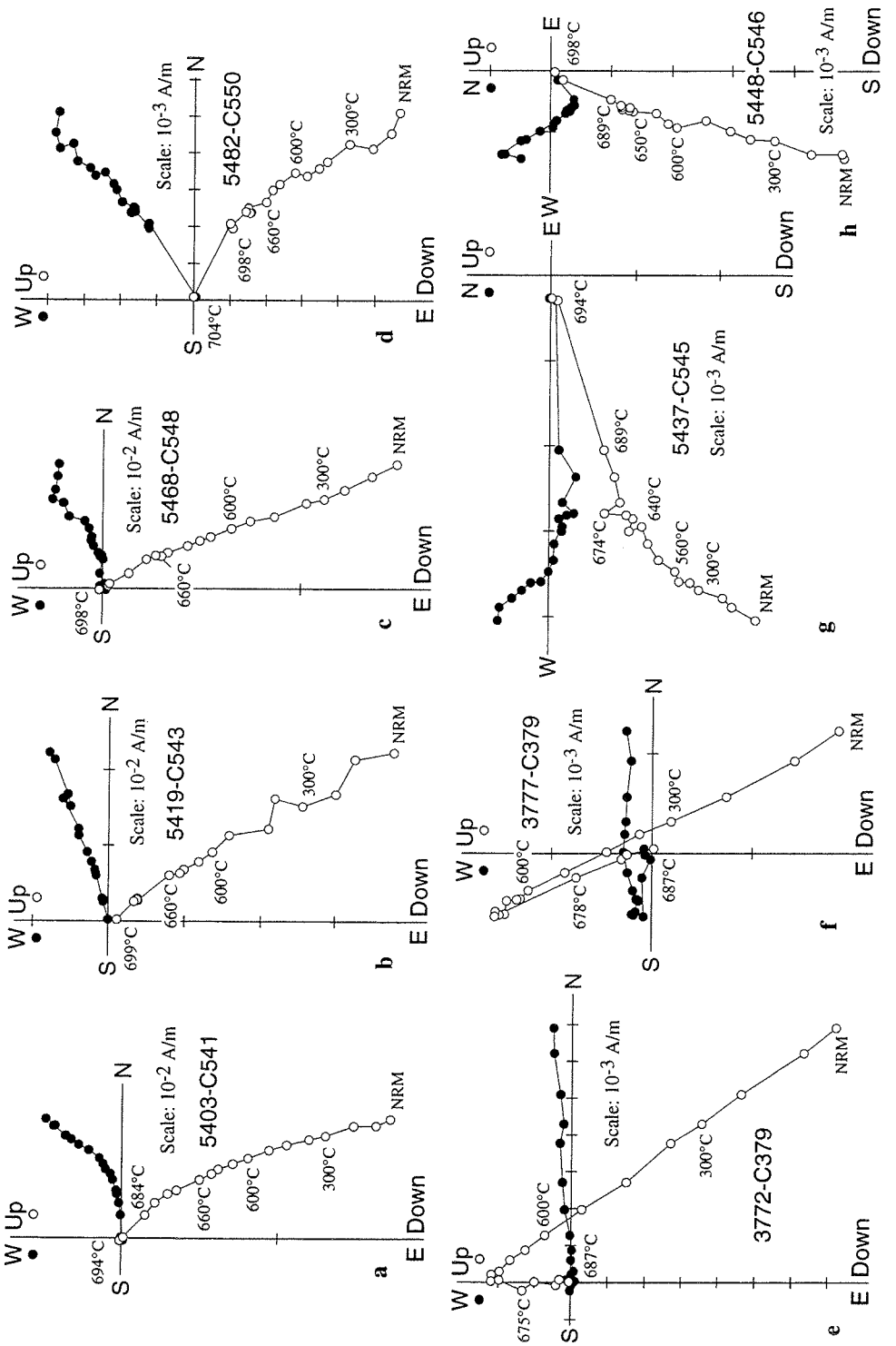

Figure 4. Thermal demagnetization diagrams of samples from the T2 Tongtoujian Formation (in situ coordinates): (a to f) from area A, (g and h) from area B.

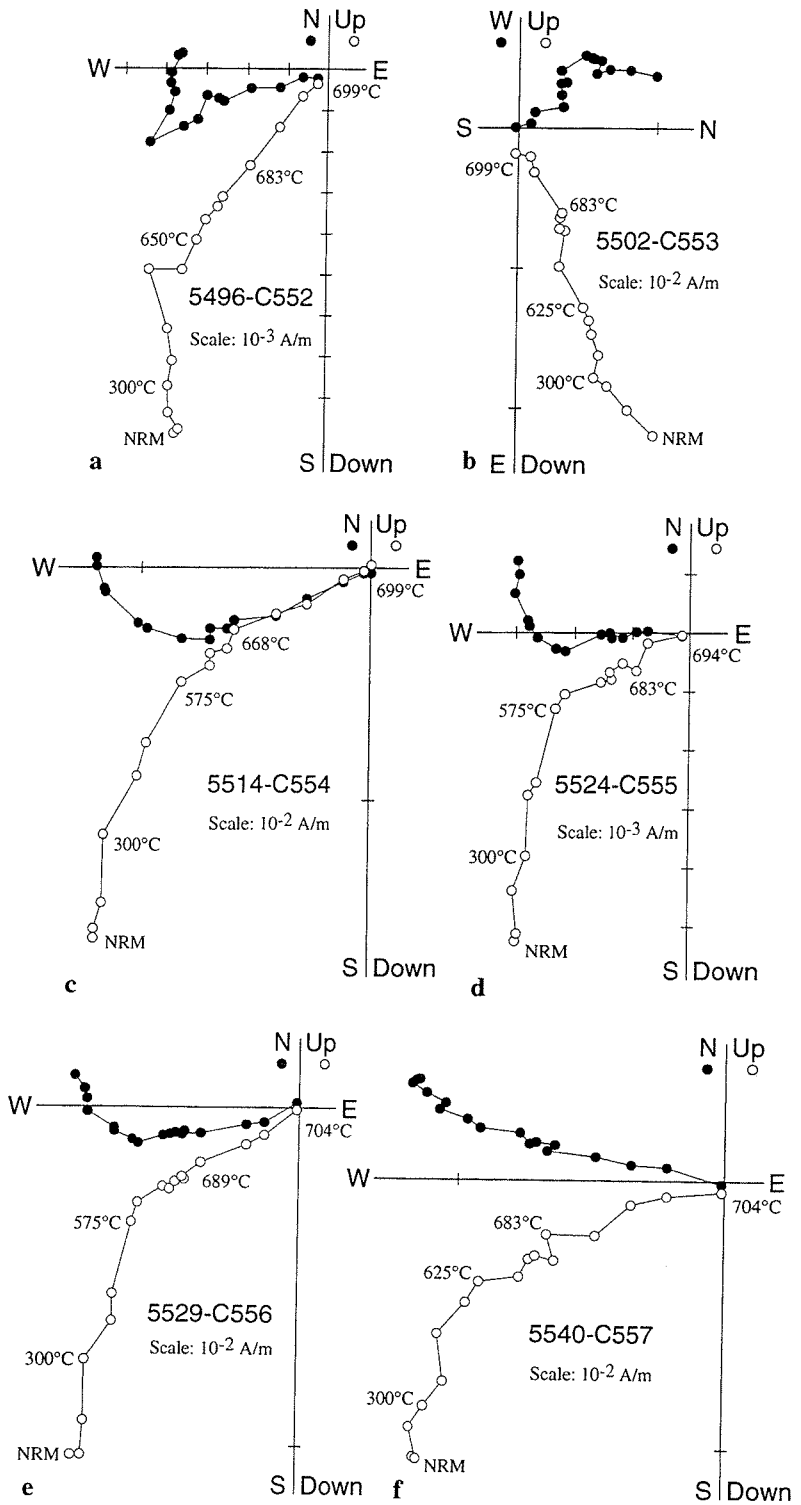

Figure 5. Thermal demagnetization diagrams of samples from the T2 Tongtoujian Formation (area C) (in situ coordinates).

The concentration parameter of the nine LTC site mean directions is greatest at 18±12% unfolding with an overall mean direction at 0% unfolding of D=339°, I=63° (k=100, α_{95}=5°). For the HTC, the concentration parameter of the nine site mean directions maximizes at 68±16% unfolding. The reversals test is positive at 95% confidence limits [*McFadden and McElhinny*, 1990].

Because only two sites were sampled at area B, statistics were treated on the sample level [*McElhinny*, 1964]. As above, two characteristic components were isolated (Figures 4g and 4h). The precision parameter (k) of the LTC based on 17 samples maximizes at 90% unfolding and yields an inconclusive fold test at the 95% significance level (ks/kg=1.44). The LTC direction at

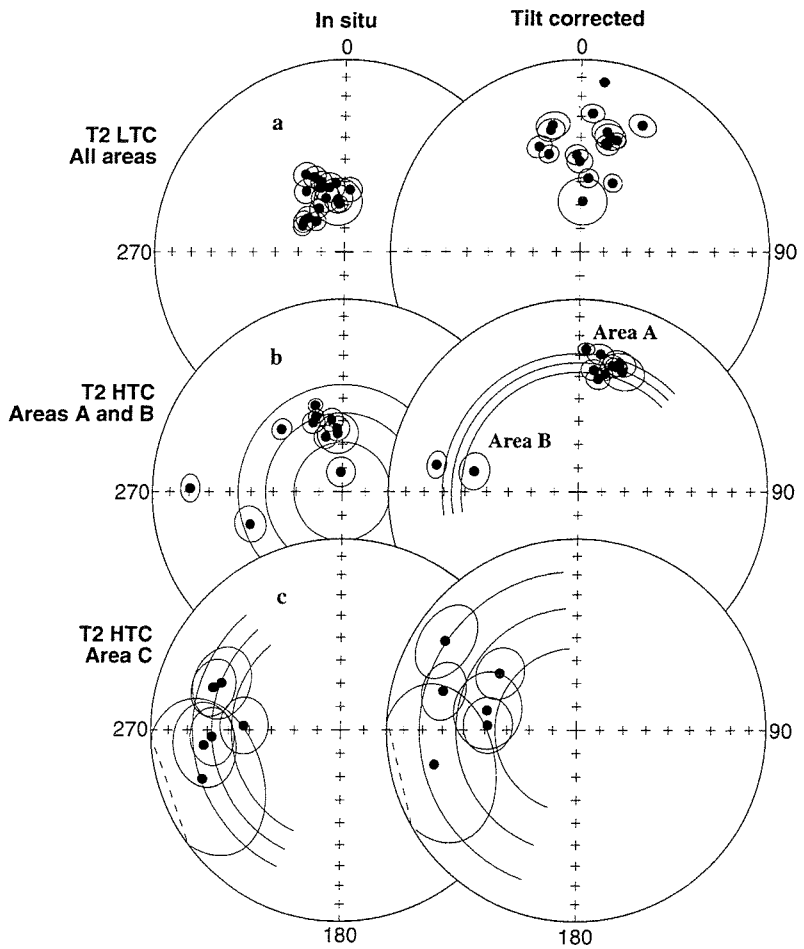

Figure 6. Equal area stereonet plots of (a) 17 site LTC mean directions from all three T2 areas, (b) 11 site HTC mean directions from T2 areas A and B, (c) 6 site HTC mean directions from T2 area C, before and after tilt correction (0 and 100% unfolding).

90% unfolding is D=346°, I=36°, k=86, α_{95}=4°; at 0% unfolding it is D=339°, I=58°, k=59, α_{95}=5°. For the HTC (Table 1), k is greatest at 100% unfolding, and the fold test is positive at 95% confidence limits.

Two characteristic components were isolated in the six sites from area C (Figure 5), however the intrasite directions are about twice as dispersed as those from the other two areas (Table 1). The LTC concentration parameter maximizes at 27±14% unfolding, with a 0% unfolding direction of D=331°, I=70° (k=71, α_{95}=8°). For the HTC, the maximum concentration parameter occurs at 2±35% unfolding.

The LTC and HTC site mean directions are plotted in Figure 6. Because the LTC site mean postfolding directions were similar among the three areas, we combined them all (N=17) to calculate an overall LTC mean direction (D=337°, I=65°, k=76, α_{95}=4°, Figure 6a). The concentration parameter maximizes at 9±8% unfolding and is clearly a postfolding component. Other steep overprints were found by several workers in Paleozoic rocks from nearby Subei Province [*Opdyke et al.*, 1986; *Kent et al.*, 1987; *Zhao*, 1987; *Wang and Van der Voo*, 1993].

As for the HTCs, the concentration parameter maximum at 68±16% unfolding for area A may be interpreted in three ways: (1) a synfolding magnetization, (2) an improper tilt correction due to a plunging fold axis, or (3) blending of the LTC and HTC components. The second possibility was tested by applying a two-step unfolding procedure that corrected for the plunging fold axis before unfolding about a horizontal axis. The fold axis of the nine bedding attitudes is N010°34° (2σ=10°) (again, this uncertainty is underestimated). This yielded a tilt corrected mean direction of D=6.6°, I=33.5° (k=162.2, α_{95}=4.1°), with a concentration parameter maximum at 78±21% unfolding. Although the concentration parameter is shifted closer to 100%, it is still within error of the result without correction for a plunging fold axis. At area A, the LTC direction is maximized at 18±12% unfolding, not at 0%. Because the LTC and HTC components are distinguished primarily by their inclinations, it could be that incomplete separation of the components shifted the LTC concentration parameter maximum from 0% toward 100% and for that of the HTC from 100% toward 0% unfolding. Although uncertain, either factors (tilt axis correction or blended magnetic components) could contribute to the apparent syn-folding result.

Because the area B HTC precision parameter maximizes at 100% unfolding, the magnetization is most probably prefolding. We thus performed the fold test on the

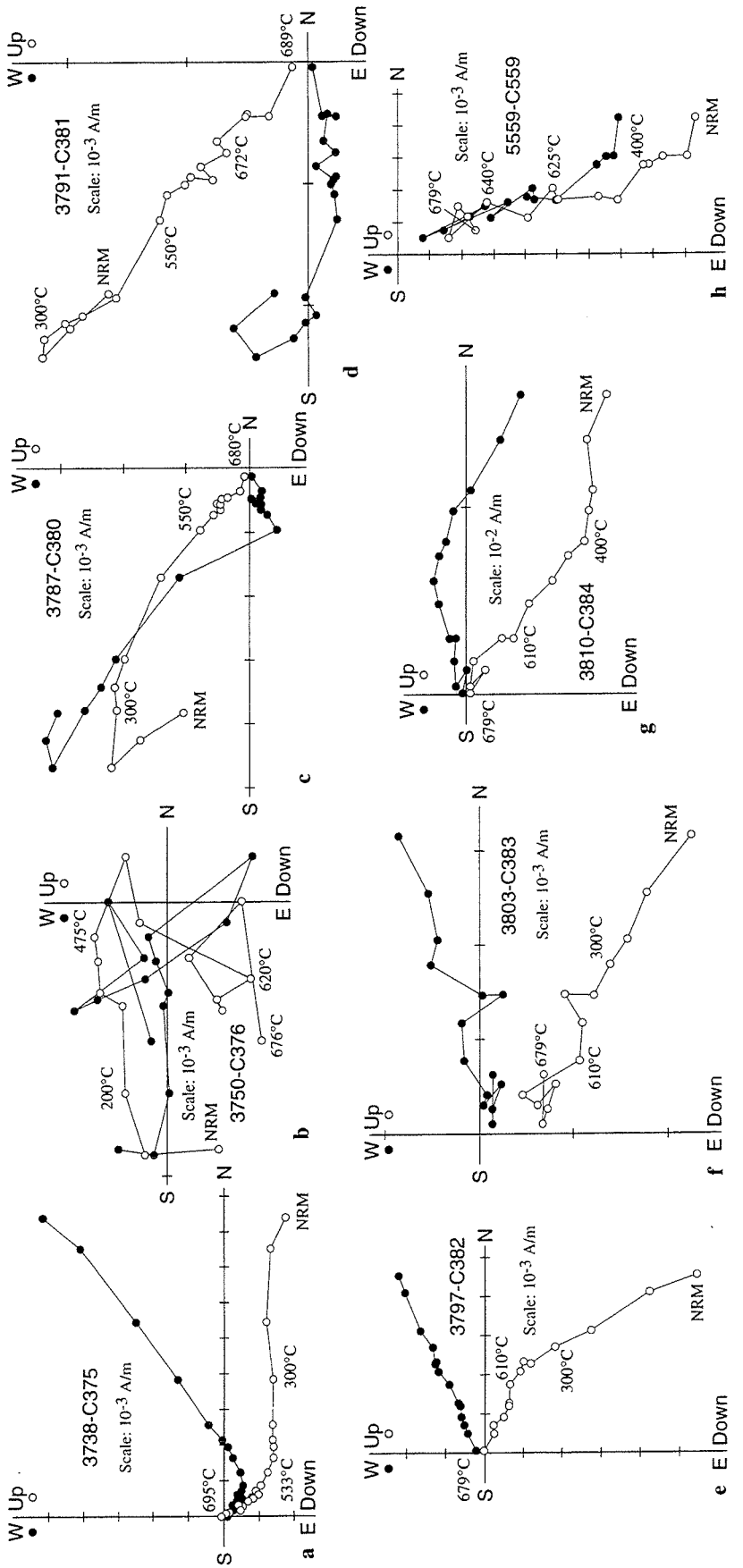

Figure 7. Thermal demagnetization diagrams of K2-E1 samples from Anhui Province (in situ coordinates).

inclination values from areas A and B [*McFadden and Reid*, 1982]; the concentration parameter maximizes at 92±17% unfolding (Figure 6b). This observation, together with the positive reversals test from area A, argue for prefolding remanences for both areas. Although reversed polarities were found in only one site, reversed polarities are also few in other T2 studies from South China. For example, of the 21 T2 Badong Formation sites studied by *Huang and Opdyke* [1997], four had reverse polarity. These four sites were sampled in a 20-m-thick section, which equals the thickness of the one site (C379) from this study. Taken together, the areas A and B HTCs are likely primary T2 magnetizations.

For area C, the HTC concentration parameter maximum occurs at 2±35%. Applying the fold test to account for a plunging fold axis results in an insignificant increase in k. Thus the area C HTC remanence is likely a postfolding remagnetization. In this case, folding and remagnetization probably occurred not long after deposition because the area C in situ inclination is very close to the areas A and B tilt-corrected inclination (Table 1).

3.1.2. Upper Cretaceous to lower Cenozoic. The demagnetization characteristics varied among the 10 sampled sites (Figure 7). High unblocking temperatures (~680°C) and red pigments of the rocks suggest the magnetic carrier was hematite in each case. Site C375 had two magnetic components (Figure 7a): a LTC in the 100°-400°C unblocking range and a HTC in the 600°-690°C unblocking range. The LTC was distinguished by equatorial inclinations and dispersed declinations, while the HTC was relatively well defined. Sites C376 and C377 (Figure 7b) had shallow LTC inclinations similar to C375 in the 100°-620°C spectra, but the magnetization became noisy at high temperatures and no HTC could be defined. For sites C380 and C381, consistent LTCs were not well defined, but reversed polarity HTCs (590°-680°C) were (Figures 7c and 7d). Two components were isolated in site C382 (Figure 7e): a LTC (25° to 500°-600°C) (D=349°, I=56°, k=129, α_{95}=5°) and a more scattered HTC (500°-690°C) (Table 1). Samples from site C383 had one consistent north and down directed magnetic component that persisted from low temperatures to 680°C yet did not decay to the origin (Figure 7f). We systematically picked the same temperature steps, never forcing to the origin, to define the characteristic component from this site. C384 behaved similarly to C383 except some samples had a northeast and down directed LTC (25°-300°C) before yielding to a north and down direction at higher temperatures that usually persisted to 680°C (Figure 7g). Site C385 had noisy magnetizations and was rejected. Site C559 had a consistent east and down direction in all samples that persisted from 200°-500°C to 680°C (Figure 7h).

The HTC concentration parameter maximizes at 90±15% unfolding (Figure 8) and the reversals test is positive at 95% confidence limits [*McFadden and McElhinny*, 1990], suggesting the HTC represents a primary K2 to E1 remanence.

3.2. Shandong Province

The bulk of area I sites come from around Wulian city. Two sites (C610 and C611) lie within the Tan-Lu fault zone and are loosely grouped into area I. Although not all the rocks are red, all of them had at least one well-defined component (Table 2) with unblocking temperatures (>650°C) suggestive of hematite as the carrier of the remanence. Site C601 had one predominant northeast and down component in the 400°-690°C unblocking range after cleaning away a randomly oriented, although mostly north and down LTC (Figure 9a). Sites C602 and C603 were collected in close proximity and their magnetizations were similar. After a few demagnetization steps, a well-defined north and down component decayed to the origin at higher temperatures (400°-680°C) (Figure 9b). Samples from site C604 had northwest and down directed components that did or did not decay to the origin. Two samples had southwest and up directions at high unblocking temperatures after removing a northwest and down component (Figure 9c). The reversed directions were not antipodal to the normal polarity population. One

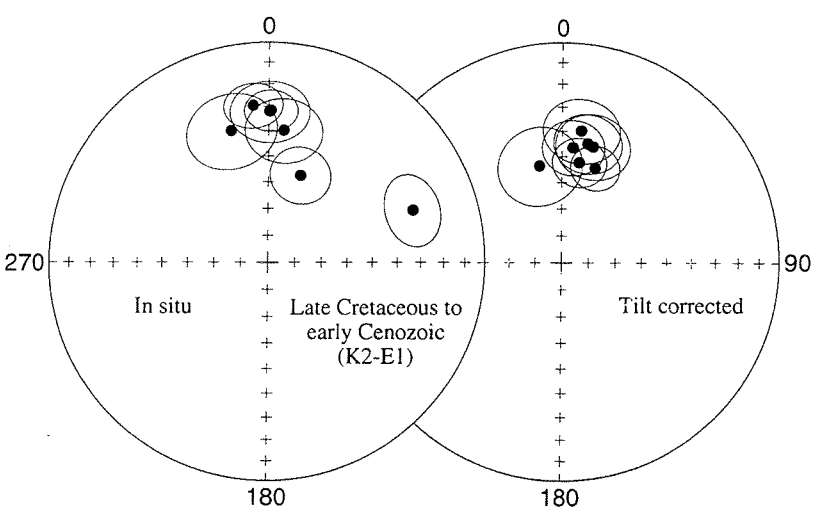

Figure 8. Equal area stereonet plots of the K2-E1 site HTC mean directions from Anhui Province, before and after tilt correction (0 and 100% unfolding).

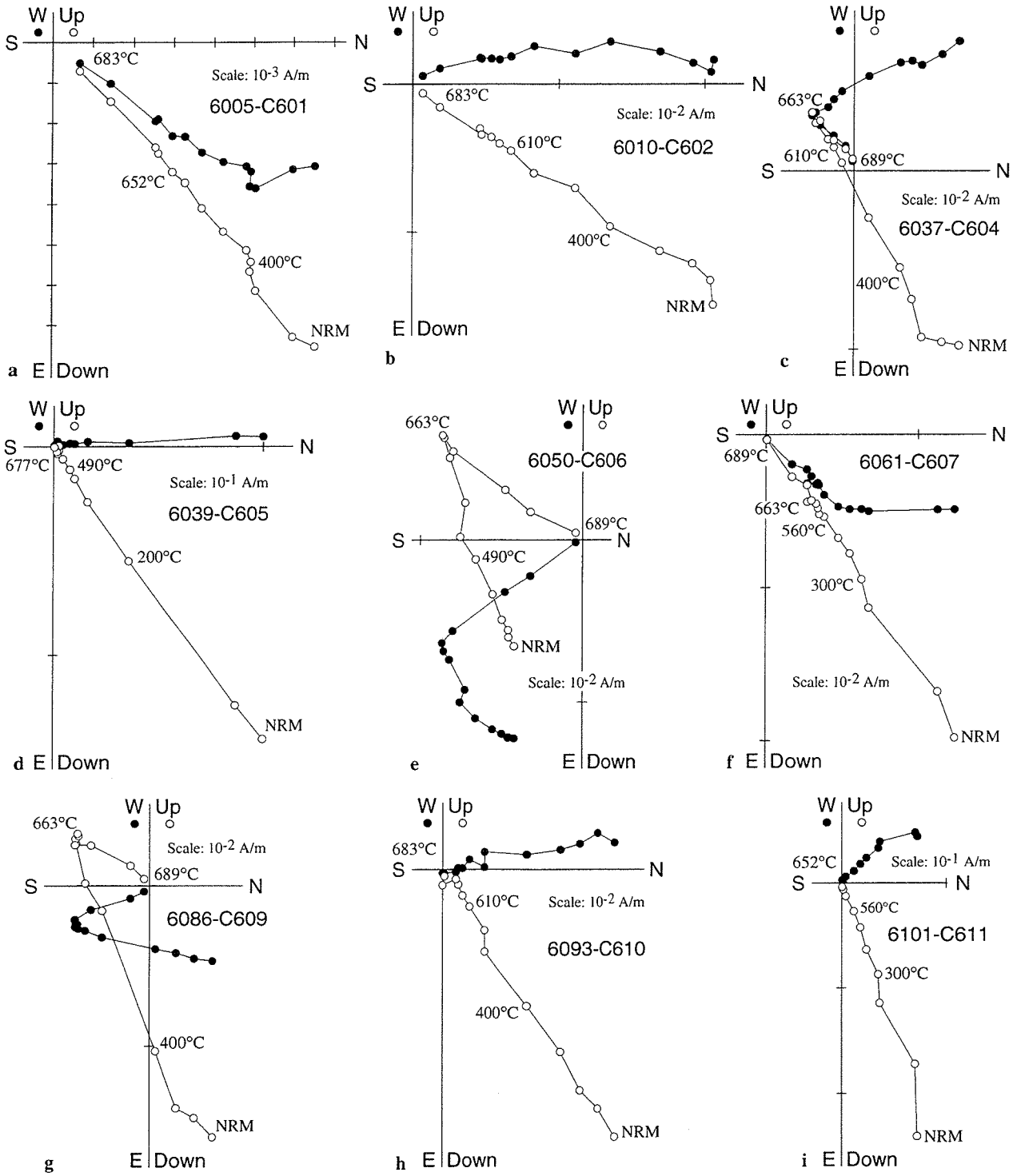

Figure 9. Thermal demagnetization diagrams of Cretaceous samples from area I, Shandong Province (in situ coordinates).

well-defined north and down component was isolated in the samples from C605 (Figure 9d). Besides hematite, an iron hydroxide was likely present as magnetic intensity drops more than 50% in the first 200°C. Sites C606 and C608 are closely spaced and their magnetizations were similar. Both had a component in the 400°-660°C temperature range (C606: D=42°, I=67°, k=122, α_{95}=4°; C608: D=57°, I=66°, k=698, α_{95}=2°) which trended to a reversed polarity component at high temperatures (660°-690°C) (Table 2, Figure 9e). C607 also had two components with a north to northeast and down LTC (25°-500°C) and a northeast and down HTC (670°-690°C) (Figure 9f). Slightly different bedding attitudes at this site allowed us to apply the fold test [*McElhinny*, 1964], which was inconclusive at 95% confidence limits. Clustering (k) decreases after tilt correction by 32%. Site

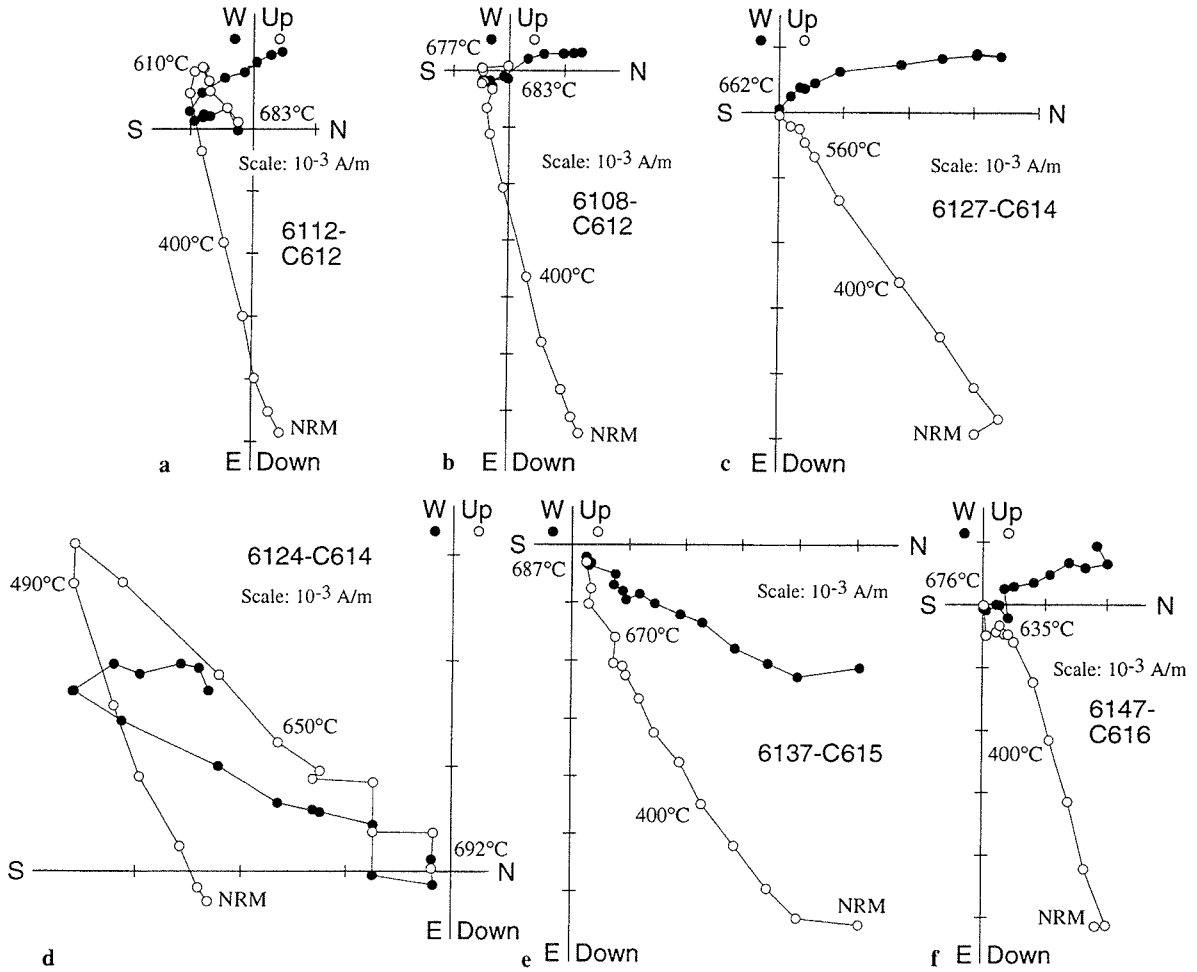

Figure 10. Thermal demagnetization diagrams of Upper Jurassic samples from area II, Shandong Province (in situ coordinates).

C609 had two magnetic components: a LTC (200°-610°C) that did not decay to the origin (D=14°, I=64°, k=629, α_{95}=2°) and a reversed polarity HTC (650°-690°C) (Figure 9g, Table 2). Only one component existed in C610; it spanned the 200°-690°C temperature range (Figure 9h, Table 2). Site C611 also had one magnetic component, which was northwest and down (Figure 9i, Table 2). A total of 90% of the magnetization decayed by 600°C, while the remaining 10% persisted to hematite unblocking temperatures.

Demagnetization characteristics from area II varied on the inter-site level. Sites C612 and C613 contained dual polarity components (Figure 10a, Table 2). The majority of the samples trended toward reversed directions then "died out" at high temperatures (Figure 10b). These latter samples were fit with great circles to define a characteristic component. Site C614 contained dual polarity magnetizations (Figures 10c and 10d). The HTC directions were quite scattered (Table 2), and a positive reversals test at 95% significance was due to a large uncertainty on both populations. All samples from site C615 had a north and down component (Figure 10e) that was taken to be the characteristic HTC (Table 2). Samples from site C616 displayed one normal polarity component with unblocking temperatures from 300° to 680°C (Figure 10f).

Both Triassic and Upper Jurassic samples were collected in area III. For the Triassic, site C617 had one north and down component (300°-680°C) after removing a viscous magnetization in the first few demagnetization steps (Figure 11a). Sites C621 and C622 were similar in that all samples had a north-northeast and down directed component in the 200°-635°C range that usually did not decay to the origin (Figure 11b). Site C623 exhibited two magnetic components: a LTC (200°-610°C) which did not decay toward the origin (D=33°, I=64°, k=188, α_{95}=4°) and a HTC (640°-680°C) which did (Figure 11c, Table 2). Samples from site C624 had a north-northeast and down directed component that did not decay to the origin in the 300°-610°C range (Figure 11d). A total of 90% of the remanence was removed by 610°C, thereafter the magnetization became unstable.

Upper Jurassic samples from area III had well defined, stable magnetizations on the whole. Those from sites C618 and C619 had northeast and down directed HTCs (300°-500° to 680°C) that decayed to the origin (Figures 12a and 12b). Common to all samples from site C620 was a northeast and down directed component (Figure 12c). A

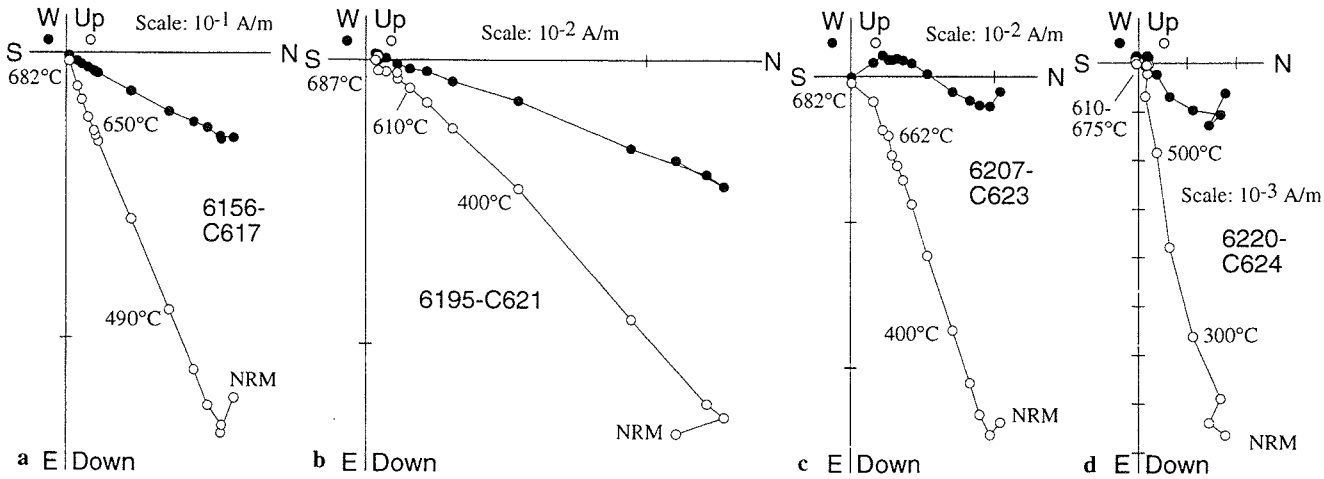

Figure 11. Thermal demagnetization diagrams of Triassic samples from area III, Shandong Province (in situ coordinates).

few samples from this site had complex, multicomponent behavior. All samples from site C627 defined northwest and down directions which did or did not decay to the origin (Figure 12d). Those from C628 had two magnetic components: a northwest and down LTC (D=300°, I=60°, k=257, α_{95}=3°), and a dual-polarity HTC (Table 2) that passed the reversals test at 95% confidence (Figure 12e). Site C629 also had two magnetic components: a LTC (100°-600°C) all with normal polarities (D=298°, I=58°, k=268, α_{95}=4°) and a HTC (657°-680°C) all with reversed polarities (Table 2, Figure 12f).

Most of the sites from area IV yielded easily

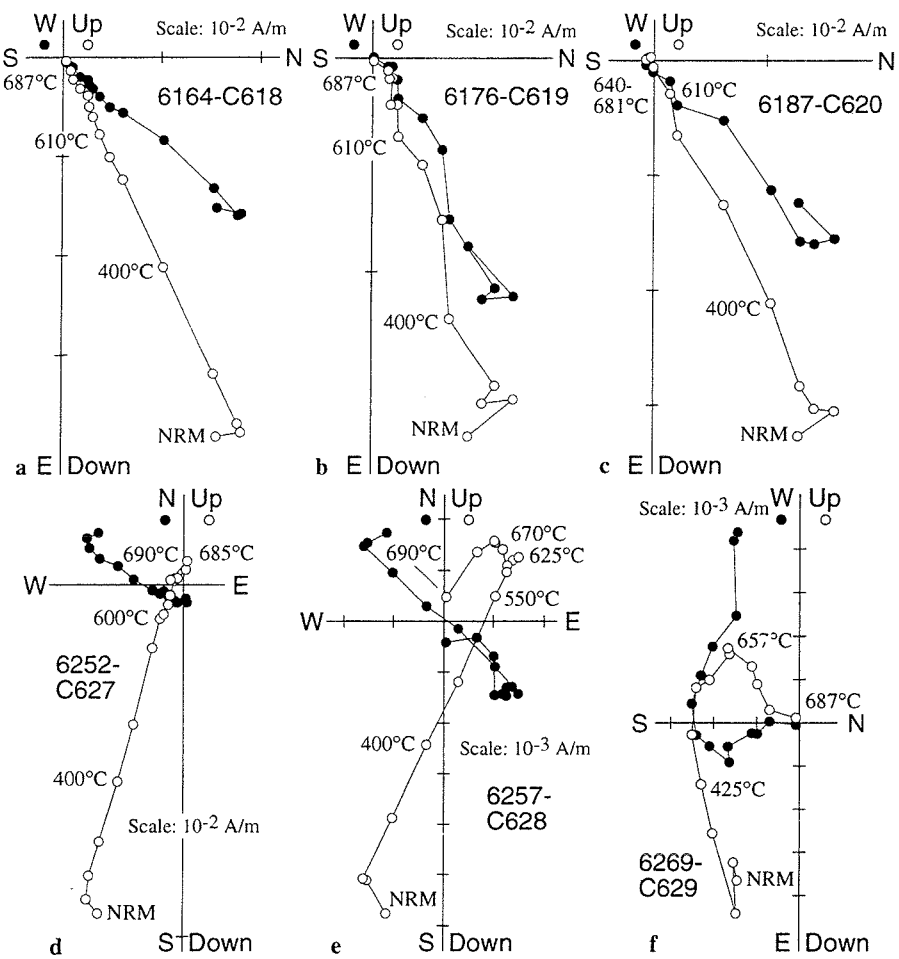

Figure 12. Thermal demagnetization diagrams of Late Jurassic samples from area III, Shandong Province (in situ coordinates).

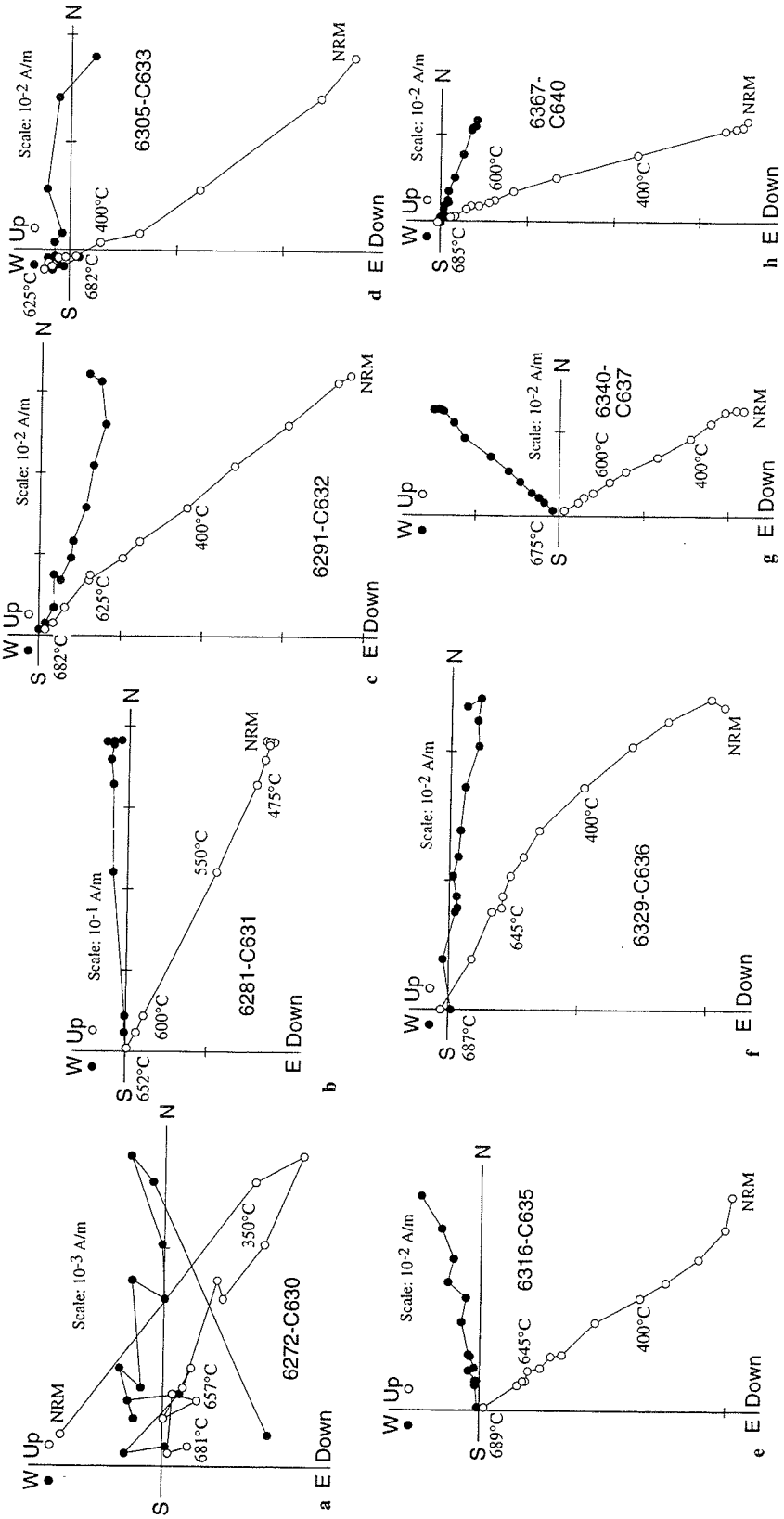

Figure 13. Thermal demagnetization diagrams of Cretaceous samples from area IV, Shandong Province (in situ coordinates).

interpretable demagnetization data (Table 2). C630 had a somewhat noisy but well defined north and down component in the 275-680°C range (Figure 13a). C631 is a ~8-m-thick ignimbrite flow with a north-northwest and down direction defined between 400° and 650°C (Figure 13b). Like the red beds, the magnetic carrier in the ignimbrite was hematite. C632 had a well defined north-northeast and down HTC (560°-680°C) (Figure 13c). C633 had a LTC (100°-560°C) of D=356°, I=54° (k=102, α_{95}=5°). During progressive unblocking the LTC trended toward a reversed direction, then became noisy as most of the remanence decayed away. Great circles were fit to all but two samples (Figure 13d) to define this component (Table 2). Site C634 had a dominant northwest and down component, as did C635 (Figure 13e). C636 had two magnetic components: a LTC (100-400°C) (D=6°, I=55°, k=272, α_{95}=3°) and a HTC (400°-680°C) which had similar declinations but shallower inclinations than the LTC (Figure 13f, Table 2). Sites C637 to C639 had a well defined northwest and down directed HTC (400°-680°C) (Figure 13g, Table 2). C640 had a well defined north-northeast and down directed HTC (300°-680°C) (Figure 13h, Table 2).

A summary of the results by area is shown in Figure 14. For Shandong, the expected present day field (PDF) direction is D=354°, I=52° and the geocentric axial dipole direction is D=0°, I=55°. With this in mind, for area I, site C610 can be quickly omitted from further consideration because its in situ direction is close to the PDF direction while the tilt corrected direction is too steep to bear tectonic significance. The other 10 site mean directions are shown in Figure 14a. The dispersion both before and after unfolding makes interpretation difficult. Some sites with northwest declinations cluster better after tilt correction than before. Site C607 fails an internal fold test and could be remagnetized. For the 10 sites, k slightly increases from 10.7 to 12.6 with a concentration parameter maximum at 60±16% unfolding. Site C611 from within the Tan-Lu fault is equally perplexing in that, if it is overprinted, it is rotated counterclockwise, but if its magnetization is primary, it is rotated clockwise versus the bulk of the site mean directions (Table 2). It is possible that local tectonics has disturbed area I. More sampling is required to understand the paleomagnetism of this area.

The small differences in bedding attitudes amongst the five sites from area II provide a mediocre situation to apply the fold test (Figure 14b). This is obvious in the error about the concentration parameter which maximizes at 66±68% unfolding. Thus the fold test provides little insight on the relative timing of magnetization. However, the reversals test is positive at 95% confidence and the precision parameter (k) doubles after tilt correction; thus the tilt corrected HTC likely represents a primary magnetization.

The Triassic from area III has a concentration parameter maximum at 15±55% unfolding (Figure 14c) and all the directions are solely of normal polarity (Table 2). The HTC magnetization of these rocks is likely postfolding. For the Late Jurassic (area III, Figure 14d), the concentration parameter maximizes at 95±15% unfolding and the reversals test is positive at the 95% confidence level, suggesting the mean tilt corrected direction is a primary Late Jurassic magnetization.

As for area IV, only site C631 (ignimbrite) has a tilt corrected declination oriented northwest. This direction could arise from a spot reading of the paleosecular variation of the magnetic field. Despite this, we included it with the ten other mean directions when applying the fold test; the maximum concentration parameter occurs at 96±10% unfolding (Figure 14e). The few (3%) reversed directions isolated for this area suggest most of these sediments and volcanics were deposited during the Cretaceous Long Normal superchron, and we regard the tilt corrected direction as a primary Cretaceous magnetization.

Lin [1984] and *Zhu* [1993] reported paleomagnetic data from Shandong Province from localities similar to those of our areas I and III. For *Lin* [1984], Pilot samples were demagnetized over 7 to 12 steps while the majority were demagnetized in at least 4-5 steps using a combination of thermal and af techniques. Because the magnetic carriers are universally hematite, it is unclear how effective the demagnetization experiments were at isolating characteristic components; only two demagnetization diagrams are provided. Neither *Lin* [1984] nor *Zhu* [1993] provided bedding information; fold tests were not applied. In light of these uncertainties, together with the potential interpretation pitfalls indicated above (e.g., area I), we believe our results supersede these earlier studies.

4. Discussion

The Mesozoic to present paleomagnetic reference poles for the NCB and SCB that were recently compiled by *Gilder and Courtillot* [1997] are used here for comparison with the new data. Because the land east of the Tan-Lu fault in Anhui Province has SCB affinities [e.g., *Zhang et al.*, 1984], we compare our Middle Triassic (T2) results with the reference pole from that block (43.0°N, 214.2°E, A_{95}=7.7°). The Upper Jurassic (J3) and Cretaceous (K1+K2) poles from both the NCB and SCB are indistinguishable, and we thus compare the Anhui and Shandong data to the combined (NCB+SCB) J3 (74.9°N, 214.3°E, A_{95}=6.5°, N=4 studies), K (74.7°N, 212.5°E, A_{95}=4.2°, N=15 studies) or early Tertiary (E1) (85.4°N, 241.7°E, A_{95}=13.5°, N=3 studies) poles.

The Anhui T2 poles calculated for areas A, B, and C (C=in situ) are 73.5°N, 251.4°E (A_{95}=3.9°), 19.1°N, 39.1°E (dp/dm=3.9/6.8°), and 10.8°N, 41.3°E (A_{95}=13.2°), respectively. With respect to the T2 SCB reference pole, these areas are rotated 36.5±7.0°, 128.0±7.4°, and 136.6±12.7° counterclockwise and displaced 3.0±6.9°, 4.5±7.3°, and 3.3±12.3° south, respectively. The K2-E1 pole from Anhui is rotated 9.0±7.7° counterclockwise and 4.1±14.1° clockwise with respect to the K and E1 reference poles, respectively. The small values and differences in rotational sense likely indicate that no significant rotation has occurred. Differences in paleolatitude are insignificant (<1°) with respect to reference poles of either age.

Figure 2 shows the declinations and bedding

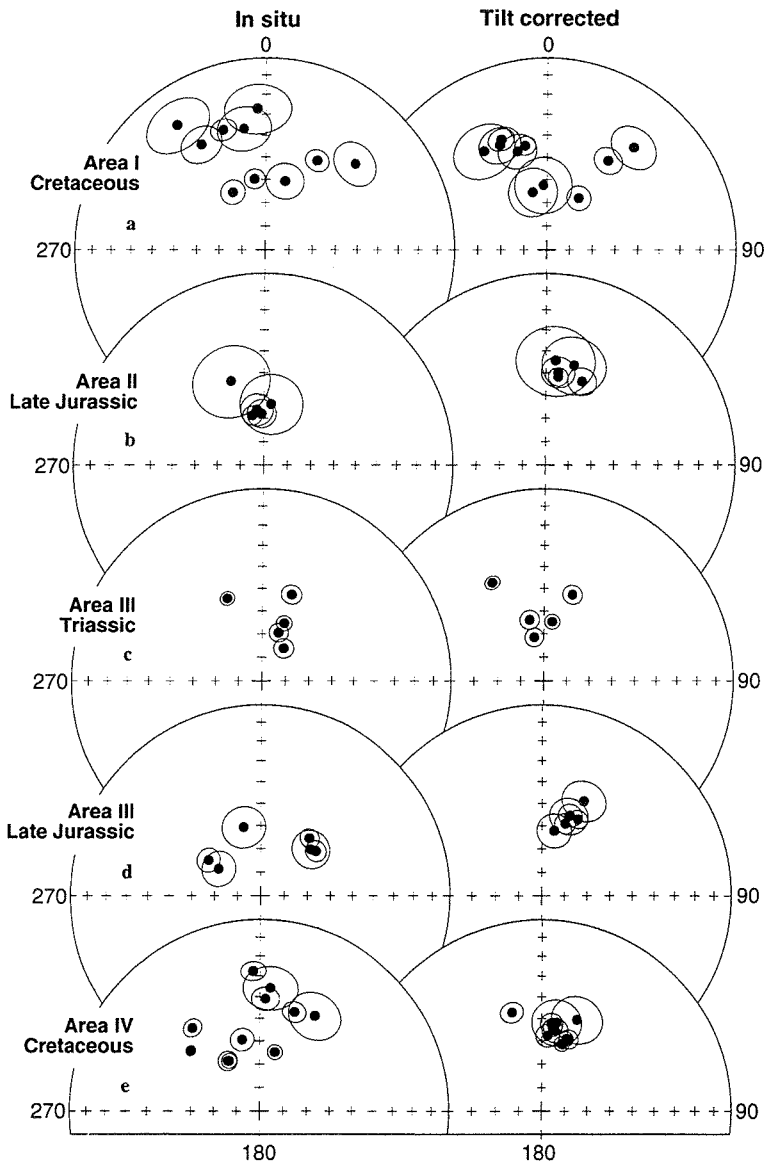

Figure 14. Equal area stereonet plots of site mean directions from Shandong Province, before and after tilt correction (0 and 100% unfolding).

information from this study together with the calculated NCB and SCB reference declinations. From the same general area east of Tan-Lu, pre-Jurassic sediments exhibit counterclockwise rotations, strike predominantly north-northwest and have plunging fold axes; post-Jurassic sediments strike northeast, exhibit no rotation and have horizontal fold axes. As NCB-SCB suturing and related deformation ended around the Middle to Late Jurassic boundary, the paleomagnetic rotations and deformation of the T2 beds are most likely associated with this collision. As noted above, the north-northwest trend of the T2 fold axes in areas A, B and C does not conform to the overall regional northeast trend of the post-T2, pre-J3 fold axes observed in southern Anhui (Figures 1 and 2). This is likely due to local tectonic effects producing more complicated deformation closer to Dabieshan and the Tan-Lu fault. Cenozoic extension best explains both the post-J3 tilting on both sides of the fault and the absence of post-J3 paleomagnetically inferred rotation.

For Shandong Province, the poles calculated for areas II (J3), III (J3), and IV (K) are 77.8°N, 235.9°E (A_{95}=6.9°), 73.5°N, 207.8°E (A_{95}=5.7°), and 81.3°N, 217.3°E (A_{95}=5.9°), respectively. With respect to the corresponding reference poles, these areas have undergone rotations of -5.6±8.8°, 2.4±8.4°, and -8.5±7.1° and latitudinal displacements of 3.4±7.6°, -1.4±6.9°, and -0.5±5.8°, respectively. Although the only result surpassing uncertainty limits is the counterclockwise rotation of area IV, its significance is doubtful. If the site C631 mean direction, which probably recorded an instantaneous (secular variation) geomagnetic field, is omitted from the overall area IV mean, the inferred rotation becomes smaller than the uncertainty.

The Shandong area II-IV mean tilt corrected declinations are shown as large arrows on Figure 3, while the area I tilt corrected site mean declinations (except C610) are indicated with small arrows. For areas II-IV, differences in rotation or paleolatitude are negligible. As

already noted, interpretation of area I directions requires more sampling and closer attention to the local geology. The lack of evidence supporting Proterozoic to Cretaceous compressional deformation was noted above. Absence of folding parallel to Tan-Lu makes it doubtful that significant shortening occurred normal to the fault in the Paleozoic or thereafter, diminishing the likelihood that this segment of Tan-Lu was once a Phanerozoic suture or paleo-subduction zone. The lack of significant folding or rotation and the concordance of paleolatitudes on both sides of the fault, coupled with the absence of Mesozoic Rb-Sr or K-Ar dates on ductile fabrics in the Tan-Lu fault zone (most are > 1.7 Ga) [*Fletcher et al.*, 1995], make the notion of Mesozoic, pluri-100 kilometer scale lateral motion along Tan-Lu fault in Shandong dubious, contrary to several existing tectonic models [e.g., *Xu et al.*, 1987; *Kimura et al.*, 1990; *Yin and Nie*, 1993; *Uchimura et al.*, 1996]. However, these observations are compatible with Late Mesozoic to Cenozoic east-west-directed extension. Although tilt axes are similar on both sides of the fault, northwest-striking normal faults cut J3-K sediments west of Tan-Lu (Figure 3), suggesting northeast directed extension acted there in the Late Cretaceous or Cenozoic; thus multiple episodes of extension are possible.

In summary, we find evidence for post-T2, pre-J3 rotation and compressive deformation east of Tan-Lu and south of Sulu. Paleolatitudes of T2 to E1 beds east of Tan-Lu are indistinguishable from those west of it. Post-J2 units have experienced neither rotation nor contractile deformation; east-west extension best explains the tectonic regime in which they were deformed. Published geologic maps and our data show that (1) post-T2, pre-J3 SCB fold axes bend around the Dabieshan metamorphic belt (Figure 1), (2) the Tan-Lu fault does not continue inside the SCB south of Dabieshan (Figure 1), and (3) a broad regional angular unconformity around the J2-J3 boundary separates times of compressive shortening below from regional extension above. South of Sulu, the Tan-Lu fault forms a plate boundary between the NCB and SCB. Counterclockwise rotation found near the fault suggests this boundary underwent left lateral shear during the NCB-SCB collision. All told, these observations are inconsistent with post-NCB-SCB collision tectonic models that invoke large strike-slip motion along the Tan-Lu fault [e.g., *Xu et al.*, 1987; *Kimura et al.*, 1990; *Uchimura et al.*, 1996]. We note that tectonic models linking large-scale motion on Tan-Lu to SCB extrusion [*Kimura et al.*, 1990; *Uchimura et al.*, 1996] are highly unlikely because the motion must be transferred from east to north, sharply curving around the Dabieshan corner, for which there is no field evidence. Furthermore, we think the potential correlations of J3 and K1 sedimentary sections [*Chen*, 1993] described above do not/cannot constrain how much, if, or when displacement occurred.

4.1. Tectonic Model

We have used the above constraints to produce a tectonic model that invokes two successive episodes of continental collision and indentation; the first being the NCB-SCB collision, and the second the India-Asia collision (Figure 15). For the first collision, *Zhao and Coe* [1989] discussed the possible Euler pole locations compatible with the NCB and SCB Permo-Triassic paleomagnetic data. Potential Euler poles lie along a great circle that bisects the paleomagnetic poles. The preferred Euler pole position should lie on the bisector at a latitude similar to Dabieshan because Euler poles lying farther north or south imply exceedingly high (up to 23,000 km) and unlikely displacements along the Qinling-Dabieshan zone [*Zhao and Coe*, 1989].

Assuming Tan-Lu acted as a transform fault during NCB-SCB collision, we can further constrain the Euler pole location (Figures 15a to 15c). If the pole lies farther south than we have placed it, Tan-Lu would function as a spreading center, for which we see no evidence (e.g., no bimodal volcanism, etc.); if the pole lies farther north, convergence would occur perpendicular to Tan-Lu, contradicting the observed deformation patterns. There is considerable leeway in placing the longitudinal position of the Euler pole, with uncertainties being >20°. One limiting factor is that the pole should not lie closer than ~4°E of Tan-Lu because anything closer would cause extension north of the Euler pole. Thus, the most likely Euler pole position is normal to the Tan-Lu fault, at least 4°E of it. The longitudinal position of the Euler pole also helps constrain the amount of displacement along Tan-Lu. For example, 60° of rotation about an Euler pole lying 500 km from Tan-Lu requires ~500 km of offset along Tan-Lu; 60° of rotation about a pole 1000 km away necessitates ~1000 km of offset. Because at least 70° of relative rotation took place between the two plates [*Zhao and Coe*, 1987], 500 km is a minimum estimate for the amount of Tan-Lu motion. Maximum estimates exceed 1000 km.

Figures 15a and 15b are alternative models (shown at different times) of the NCB-SCB collision based on the paleomagnetic database. Figure 15a shows the configuration of the NCB and SCB during the Early to Middle Triassic. Note that the SCB margin does not resemble the present one, while that for the NCB does. If the Euler pole was positioned as it is in Figure 15a, both Tan-Lu and Sulu lie on the same small circle about the pole, suggesting that they acted as a continuous transform structure. On the other hand, if the pole was positioned farther east (Figure 15b), convergence would occur in the Sulu area while Tan-Lu would function as a strike-slip fault. In this case, two subduction zones, which lay where the UHP metamorphic rocks presently crop out (Qinling-Dabieshan and Sulu), would be separated by the Tan-Lu transform fault. Creation and exhumation of the eclogite-bearing metamorphic terranes would occur in situ, possibly experiencing minor lateral offset due to obliquity of the subduction geometry. With either model shown in Figures 15a or 15b, UHP rocks originally generated and exhumed near Dabieshan could have been transported along Tan-Lu, eventually arriving in the Sulu area via plate capture, like Baja California began moving northward relative to North America upon transfer from it to the Pacific plate around 5.5 Ma [*Atwater*, 1989].

The Dabieshan corner began indenting the SCB in the Late Triassic (Figure 15b), and the Tan-Lu fault grew within the SCB as Dabieshan continued indenting the SCB. Indentation of the SCB by the NCB was also suggested by *Okay et al.* [1993] and *Eide* [1995]. Folding of the SCB cover strata conformed to the NCB margin as suturing continued in the Middle Jurassic (Figure 15c). It is most probable that the Mesozoic deformation

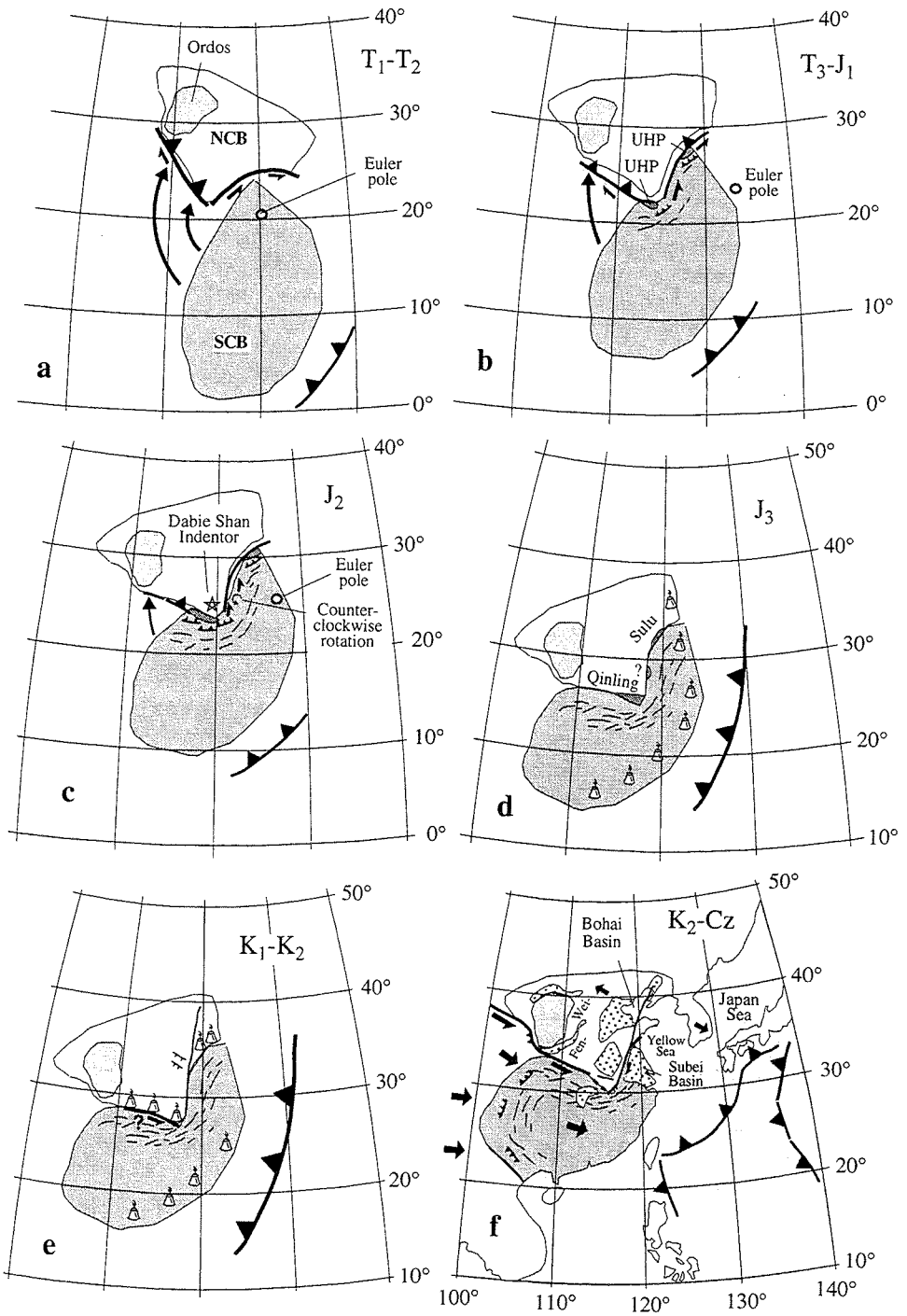

Figure 15. Tectonic model of the Tan-Lu fault from the Mesozoic to present. Tectonic interpretations span the geologic epochs indicated in each frame. Note that Figures 15a and 15b are alternative models. In either case, UHP rocks originally exhumed near Dabieshan could have been transported by plate capture toward Sulu along Tan-Lu through the Middle Jurassic (Figure 15c). (a) Early to Middle Triassic: SCB rotates clockwise with respect to the NCB; Tan-Lu acts as a transform fault. (b) Late Triassic to Early Jurassic: UHP metamorphic rocks are exhumed in Qinling-Dabieshan and Sulu. The Dabieshan corner begins impinging the SCB. Folding and faulting of the SCB cover strata begins. Tan-Lu becomes a continental shear zone. (c) Middle Jurassic: Active continental collision continues deforming the SCB. Tan-Lu grows in the SCB as Dabieshan advances. Local counterclockwise rotations occur near the Tan-Lu shear zone. (d) Late Jurassic: The NCB-SCB collision is completed. Eastward subduction of the proto-Pacific commences. The region experiences plutonism and volcanism. (e) Early-Late Cretaceous: Volcanism related to subduction continues near the coast due to subduction. Obliquity of the subducting plate changes during this time, possibly resulting in minor lateral offset along Tan-Lu and related faults. Circa 125 Ma granites form along Qinling, Sulu, and along the eastern margin of China. (f) Late Cretaceous to Cenozoic: Extrusion of the SCB occurs under the influence of the India-Asia collision. Escape of the SCB is accommodated along lateral faults in the Qinling suture which sole out in various normal faults and extensional basins. Note that the Tan-Lu fault now cuts the NCB north of Sulu. North-trending folds in the Sichuan Basin (SCB) are the result of this new phase of deformation.

documented by *Hsü et al.* [1988], from places lying only 100 to 200 km south and east of Dabieshan, was related to the NCB-SCB collision and not to some other. Note that the Middle Jurassic reconstruction was made by smoothing the discrepancy of the paleolatitudinal component in the two APWP curves while respecting the rotational component [*Gilder and Courtillot*, 1997].

A potential pitfall of this model is that some U-Pb dates of UHP rocks are T1 and T2, yet Figure 15a shows that the two continents were not in contact. It is not clear whether continent-continent collision is a necessary condition to produce UHP material. Sediments shed off the SCB could have been subducted to UHP conditions before the two plates were in contact near Dabieshan. Alternatively, we do not know the original shape of the SCB. It is possible that the northern margin of SCB extended farther northwest than depicted, in which case continental collision could commence as early as the Early Triassic in Dabieshan. This would also explain the lack of direct evidence for oceanic subduction at that time along the Qinling-Dabieshan zone (no Mesozoic ophiolites, post-T3 marine sediments nor post T1, pre-J3 volcanics).

After this first (NCB-SCB) collision ended, widespread volcanism and plutonism occurred in eastern China in the Late Jurassic (Figure 15d) and Early Cretaceous (Figure 15e). This magmatism was probably linked to subduction of the proto-Pacific plate. Obliquity in the convergence angle could produce strike slip motion in the back arc region. It is possible that this angle changed through time, potentially producing minor (tens of km) dextral and/or sinistral offset on Tan-Lu and related faults. This would account for the 99±2 Ma mylonites described above. A tectonic explanation for the circa 125 Ma volcanism and plutonism along the Qinling-Dabieshan and Sulu belts (Figure 15e) is enigmatic. It is doubtful that the genesis of these Lower Cretaceous Qinling-Dabieshan granites was linked to transtension along the Pacific continental margin [*Hacker et al.*, 1995] because the belt of granites is linear over a distance of ~1000 km and trends perpendicular to the margin (Figure 1). They may have been produced from melting of the thickened crust along the suture zone, which happened some 50 million years before. Initial strontium from 0.709 to 0.711 and initial epsilon neodymium from -15 to -21 of three 122 to 124 Ma intermediate to felsic intrusives suggest they were derived from a significant proportion of crustal material [*Chen and Jahn*, 1998]. Delays of tens of millions of years between a crustal thickening event and subsequent melting are possible, depending on the geometry of thickening, erosion parameters, conductivity of the lithosphere, etc. [e.g., *England and Thompson*, 1984; *Thompson and Connolly*, 1995]. However, two-dimensional models suggest that collapsed mountain chains producing crustal melts are generally wider than 300 km [*Gaudemer et al.*, 1988]. This is not the case for the Qinling-Dabieshan belt where the zone of granites is long and narrow (Figure 1). Thus melting related to strike-slip activity may be favored over postcollision collapse. Consistent with this idea, *Reischmann et al.* [1990] described an east-west-trending ductile shear zone with sinistral kinematic indicators in the Qinling Mountains south of Xi'an. A two-point Sm-Nd isochron from the mylonite in the shear zone yields 126±9 Ma. However, it is not clear why strike-slip activity occurred at this time in the Qinling nor is it apparent that the duration and magnitude of displacement needed to produce the granites from strike-slip motion took place [e.g., *Leloup et al.*, 1999]. Finally, the circa 125 Ma Sulu granites may not be related in a tectonic sense to those in Qinling. Sulu granites could be related to proto-Pacific plate subduction, like the ~125 Ma granites that crop out in the southeastern SCB.

Of the hypotheses that could explain Cenozoic east-west extension, we prefer the model of SCB extrusion related to the India-Asia collision for several reasons. First, extrusion tectonics are documented. Estimates from active faulting suggest left lateral movement of the SCB with respect to Gobi-Mongolia is presently 12±4 mm/yr [*Zhang et al.*, 1995]. Cenozoic left-lateral displacement found on a single fault in the Qinling belt could be as high as 150 km [*Peltzer et al.*, 1985]. Second, the position of Cenozoic basins in east China strongly support this hypothesis [e.g., *Tapponnier et al.*, 1982]. With the exception of the Jianghan basin, the major basins with appreciable Cenozoic fill in eastern China (Subei, Yellow Sea, and Bohai) are located north of the Qinling belt (Figure 1). In the Yellow Sea, ridges and basins (and magnetic anomalies) possess the same northeast-trend as the Fen-Wei grabens farther inland [*Wageman et al.*, 1970]. If the SCB did extrude east relative to the NCB, by analogy we should expect basins to form north of the extruding block, just as the South China Sea opened in response to the extrusion of Sundaland [e.g., *Briais et al.*, 1993]. This appears to be the case. Finally, post-Early Cretaceous compressive deformation in the western SCB is widespread in Yunnan, Sichuan, Guangxi, and Guizhou provinces [*Opdyke et al.*, 1986; *Tapponnier et al.*, 1986; *Enkin et al.*, 1991; *Leloup*, 1991; *Gilder et al.*, 1993, 1995] (see also provincial geologic compilations from Yunnan, Sichuan, Guangxi, Guizhou, etc.).

Figure 15f presents the extrusion model related to the second collision event (India-Asia), which may have begun as early as the Late Cretaceous [*Jaeger et al.*, 1989] and still continues today. Left lateral faults trend along the Qinling-Dabieshan suture; however, none cut the SCB east of the Tan-Lu fault. There the offset is absorbed by extension and Tan-Lu was reactivated as a right-lateral and/or normal fault, this time extending north of the older Sulu belt as predicted by numerical models for SCB extrusion [*Peltzer and Saucier*, 1996].

5. Conclusions

Rotation and folding patterns of T2 to E1 sediments in Shandong and eastern Anhui provinces suggest that sinistral shear along the Tan-Lu fault in Anhui was related to the NCB-SCB collision (collision 1). The Euler pole defining the relative motion between the two blocks was east of, and orthogonal to, Tan-Lu. Two subduction zones likely existed before and during active collision- one in Qinling-Dabieshan and the other in Sulu. The two were connected by the Tan-Lu transform fault which did not extend into the NCB, north of Sulu. Creation and exhumation of the UHP metamorphic rocks occurred in nearly the same relative positions as found today. Some

UHP material originally generated near Dabieshan may have been transported toward Sulu along Tan-Lu via plate capture. The Dabieshan area was a promontory of the NCB that acted as a rigid indenter which deformed the SCB, causing folds to wrap around the indenter. Reactivation of Tan-Lu occurred in the Late Cretaceous to Cenozoic, probably due to SCB extrusion under the influence of the India-Asia collision (collision 2), at which time the fault cut the NCB, north of Sulu.

We believe that our model supersedes previous models. Although the thin-skin model of *Li* [1994] cannot be entirely refuted by this study, we note that the proposed match of aeromagnetic anomalies is not compelling and that the deformation patterns in the proposed thin-skin area east of Tan-Lu are not consistent when compared to other places where similar models are invoked (e.g., Altyn-Tagh fault, Qaidam basin, and Qilianshan [*Meyer et al.*, 1998]). The latter models suggest fold axes east of Tan-Lu should be perpendicular (west to northwest), not parallel (north to northeast), to the convergence direction within the overthrust block; however, the preponderance of fold axes in the area east of Tan-Lu and south of Sulu trend northeast (Figures 1 and 2). Another problem with this model is that all UHP material must have been exhumed from mantle depths to <20 km before detachment occurred.

Next, the syncollision model by *Yin and Nie* [1993] neglects several key points such as the paleomagnetically inferred rotation during NCB-SCB collision. With the rotation, a SCB indenter poses an impossible space problem. Second, the NCB is the old, cold craton, which contains very ancient rock relicts (3.5-3.8 Ga), with a peak period of formation around 2.7 to 2.5 Ga [e.g., *Jahn and Zhang*, 1984; *Jahn et al.*, 1987, 1988; *Liu et al.*, 1990, 1992] that virtually escaped major Mesozoic deformation (e.g., the flat-lying Ordos basin). The SCB is relatively youthful in comparison, with a peak formation time of about 1.6 Ga [e.g., *Huang and DePaolo*, 1989; *Gilder et al.*, 1996; *Chen and Jahn*, 1998], and it was highly deformed in the Mesozoic, especially near the Qinling-Dabieshan suture zone. These observations suggest that the relatively young SCB was deformed by the older, colder NCB. A similar argument based on rheological differences was made by *Tapponnier and Molnar* [1977] for the India-Asia collision. Moreover, the SCB-indenter model requires roughly an equal amount of left lateral offset occurring on Tan-Lu north of Sulu, for which there is no firm evidence.

Much of the Asian mosaic is a composite of successive tectonic events, with younger deformations overprinting older ones. Many of the tectonic features that played key roles in the past were reactivated during the most recent episode. Understanding and describing properly the geometry and amplitude of the older events, such as the NCB-SCB collision and the role of NCB as an indenter, requires detailed understanding and description of the vast consequences of the latest tectonic event with continent wide effects, namely the India-Asia collision.

Acknowledgments. We are very grateful to Xu Jiawei, Li Shuangying, Wang Daoxuan, and Zhang Hongchun from the Hefei Institute of Technology, Anhui and Zhang Zihuan, Wang Chengpei, and Huan Xinchang from the Geological Survey in Xiaozhou, Shandong, for their participation in the field. Reviews from Bradley Hacker and Lothar Ratschbacher improved this manuscript, which benefited from computer programs written by Richard Allmendinger, Jean-Pascal Cogné, and Randy Enkin. Funding was generously provided by INSU and a NNSFC grant 49672148 to WJX. This is contribution 1603 from the Institut de Physique du Globe de Paris and 397 from the Institute of Tectonics at the University of California at Santa Cruz.

References

Academia Sinica, Geological Map of China, 1:4,000,000, Geologic Publishing House, Beijing, 1976.

Ames, L., G.R. Tilton, and G.Z. Zhou, Timing of collision of the Sino-Korean and Yangtze cratons: U-Pb zircon dating of coesite-bearing eclogites, *Geology*, *21*, 339-342, 1993.

Ames, L., G.Z. Zhou, and B.C. Xiong, Geochronology and isotopic character of ultrahigh-pressure metamorphism with implications for collision of the Sino-Korean and Yangtze cratons, central China, *Tectonics*, *15*, 472-489, 1996.

Anhui Bureau of Geology and Mineral Resources (AHBGMR), *Regional Geology of Anhui Province*, 721 pp., Geol. Publ., Beijing, 1987.

Atwater, T., Tectonic implications of post-30 Ma Pacific and North American relative plate motions, *Geol. Soc. Am. Bull.*, *107*, 937-959, 1995.

Briais, A., P. Patriat, and P. Tapponnier, Updated interpretation of magnetic anomalies and seafloor spreading stages in the South China Sea- Implications for the Tertiary tectonics of southeast Asia, *J. Geophys. Res.*, *98*, 6299-6328, 1993.

Chemenda, A.I., M. Mattauer, J. Malavieille, and A.N. Bokun, A mechanism for syn-collisional rock exhumation and associated normal faulting; results from physical modeling, *Earth Planet. Sci. Lett.*, *132*, 225-232, 1995.

Chemenda, A.I., M. Mattauer, and A.N. Bokun, Continental subduction and a mechanism for exhumation of high-pressure metamorphic rocks; new modeling and field data from Oman, *Earth Planet. Sci. Lett.*, *143*, 173-182, 1996.

Chen, J.F., and B.M. Jahn, Crustal evolution of southeastern China: Nd and Sr isotopic evidence, *Tectonophysics*, *284*, 101-133, 1998.

Chen, P.J., Timing of displacement along the Tancheng-Lujiang fault zone and the migration of Late Mesozoic volcanism in eastern China, in *The Tancheng-Lujiang Wrench Fault System*, edited by J.W. Xu, pp. 105-111, John Wiley, New York, 1993.

Chen, W.J., T.M. Harrison, M.T. Heizler, R.X. Liu, B.L. Ma, and J.L. Li, The cooling history of melange zone in north Jiangsu-south Shandong region: Evidence from multiple diffusion domain 40Ar-39Ar thermal geochronology, *Acta Petrol. Sinica*, *8*, 1-17, 1992.

Chen, W.P., and J. Nábelek, Seismogenic strike-slip faulting and the development of the north China basin, *Tectonics*, *7*, 975-989, 1988.

Eide, E.A., A model for the tectonic history of HP and UHPM regions in east central China, in *Ultrahigh Pressure Metamorphism*, edited by R.G. Coleman and X.M. Wang, pp. 391-426, Cambridge Univ. Press, Cambridge, 1995.

Eide, E.A., M.O. McWilliams, and J.G. Liou, $^{40}Ar/^{39}Ar$ geochronology and exhumation of high-pressure to ultrahigh-pressure metamorphic rocks in east-central China, *Geology*, *22*, 601-604, 1994.

Enami, M., and Q.J. Zang, Quartz pseudomorphs after coesite in eclogites from Shandong Province, east China, *Am. Mineral.*, *75*, 381-386, 1990.

England, P.C., and A.B. Thompson, Pressure-temperature-time paths of regional metamorphism, I, Heat transfer during the evolution of regions of thickened continental crust, *J. Petrol.*, *25*, 894-928, 1984.

Enkin, R.J., Y. Chen, V. Courtillot, J. Besse, L.S. Xing, Z.H. Zhang, Z.H. Zhuang, and J. Zhang, A Cretaceous pole from south China and the Mesozoic hairpin turn of the Eurasian apparent polar wander path, *J. Geophys. Res.*, *96*, 4007-4027, 1991.

Enkin, R.J., Z.Y. Yang, Y. Chen, and V. Courtillot, Paleomagnetic constraints on the geodynamic history of the major blocks of China from the Permian to the present, *J. Geophys. Res.*, *97*, 13,953-13,989, 1992.

Fisher, R.A., Dispersion on a sphere, *Proc. R. Soc. London A, 217*, 295-305, 1953.

Fletcher, C.J.N., W.R. Fitches, C.C. Rundle, and J.A. Evans, Geological and isotopic constraints on the timing of movement in the Tan-Lu fault zone, northeastern China, *J. Southeast Asian Earth Sci., 11*, 15-22, 1995.

Gaudemer, Y. C. Jaupart, and P. Tapponnier, Thermal control on post-orogenic extension in collision belts, *Earth Planet. Sci. Lett., 89*, 48-62, 1988.

Gilder, S., and V. Courtillot, Timing of the North-South China collision from new middle to late Mesozoic paleomagnetic data from the North China Block, *J. Geophys. Res., 102*, 17,713-17,727, 1997.

Gilder, S.A., G.R. Keller, M. Luo, and P.C. Goodell, Timing and spatial distribution of rifting in China, *Tectonophysics, 197*, 225-243, 1991.

Gilder, S.A., R.S. Coe, H.R. Wu, G.D. Kuang, X.X. Zhao, Q. Wu, and X.Z. Tang, Cretaceous and Tertiary paleomagnetic results from southeast China and their tectonic implications, *Earth Planet. Sci. Lett., 117*, 637-652, 1993.

Gilder, S.A., R.S. Coe, H.R. Wu, G.D. Kuang, X.X. Zhao, and Q. Wu, Triassic paleomagnetic data from southern China and their bearing on the tectonic evolution of the western circum-Pacific region, *Earth Planet. Sci. Lett., 131*, 269-287, 1995.

Gilder, S., J. Gill, R. Coe, X. Zhao, H. Liu, G. Wang, K. Yuan, W. Liu, G. Kuang, and H. Wu, Isotopic and paleomagnetic constraints on the Mesozoic tectonic evolution of south China, *J. Geophys. Res., 101*, 16,137-16,154, 1996.

Hacker, B.R., and Q.C. Wang, Ar/Ar geochronology of ultrahigh-pressure metamorphism in central China, *Tectonics, 14*, 994-1006, 1995.

Hacker, B.R., L. Ratschbacher, L. Webb, and S.W. Dong, What brought them up? Exhumation of the Dabie Shan ultrahigh-pressure rocks, *Geology, 23*, 743-746, 1995.

Hacker, B.R., L. Ratschbacher, L. Webb, T. Ireland, D. Walker, and S.W. Dong, U/Pb zircon ages constrain the architecture of the ultrahigh-pressure Qinling-Dabie orogen, China, *Earth Planet. Sci. Lett., 161*, 215-230, 1998.

Henan Bureau of Geology and Mineral Resources (HNBGMR), *Regional Geology of Henan Province*, 772 pp., Geol. Publ., Beijing, 1989.

Hirajima, T., A. Ishiwatari, B. Cong, R. Zhang, S. Banno, and T. Nozaka, Coesite from Mengzhong eclogite at Dhonghai county, northeastern Jiangsu province, China, *Mineral Mag., 54*, 579-583, 1990.

Hsü, K.J., S. Sun, J.L. Li, H.H. Chen, H.P. Pen, and A.M.C. Sengor, Mesozoic overthrust tectonics in south China, *Geology, 16*, 418-421, 1988.

Huang, X., and D.J. DePaolo, Study of sources of Paleozoic granitoids and the basement of south China by means of Nd-Sr isotopes, *Acta Petrol. Sinica, 1*, 28-36, 1989.

Huang, K.N., and N.D. Opdyke, Paleomagnetism of Middle Triassic redbeds from Hubei and northwestern Hunan provinces, South China, *Earth Planet. Sci. Lett., 143*, 63-79, 1996.

Huang, K.N., and N.D. Opdyke, Middle Triassic paleomagnetic results from central Hubei province, China and their tectonic implications, *Geophys. Res. Lett., 24*, 1571-1574, 1997.

Jaeger, J.J., V. Courtillot, and P. Tapponnier, Paleontological view of the ages of the Deccan Traps, the Cretaceous/Tertiary boundary, and the India-Asia collision, *Geology, 17*, 316-319, 1989.

Jahn, B.M., and Z.Q. Zhang, Archaean granulite gneisses from eastern Hebei Province, China: Rare earth geochemistry and tectonic implications, *Contrib. Mineral. Petrol., 85*, 224-243, 1984.

Jahn, B.M., B. Auvray, J. Cornichet, Y.L. Bai, Q.H. Shen, and D.Y. Liu, 3.5 Ga old amphibolites from eastern Hebei Province, China: Field occurrence, petrography, Sm-Nd isochron age and REE geochemistry, *Precambrian Res., 34*, 311-346, 1987.

Jahn, B.M., B. Auvray, Q.H. Shen, D.Y. Liu, Z.Q. Zhang, Y.J. Dong, X.J. Ye, Q.Z. Zhang, J. Cornichet, and J. Mac, Archaean crustal evolution in China: The Taishan complex and evidence for juvenile crustal addition from long-term depleted mantle, *Precambrian Res., 38*, 381-403, 1988.

Kent, D.V., X. Zeng, W.Y. Zhang, and N.D. Opdyke, Widespread late Mesozoic to recent remagnetization of Paleozoic and lower Triassic sedimentary rocks from south China, *Tectonophysics, 139*, 123-143, 1987.

Kimura, G, M. Takahashi, and M. Kono, Mesozoic collision-extrusion tectonics in eastern Asia, *Tectonophysics, 181*, 15-23, 1990.

Kirschvink, J.L., The least-square line and plane and the analysis of paleomagnetic data, *Geophys. J. R. Astron. Soc., 62*, 699-712, 1980.

Kröner, A., G.W. Zhang, and Y. Sun, Granulites in the Tongbai area, Qinling belt, China: Geochemistry, petrology, single zircon geochronology, and implications for the tectonic evolution of eastern Asia, *Tectonics, 12*, 245-255, 1993.

Leloup, P.H., Cinématique des Déformations "Himalayennes" dans la zone ce cisaillement crustale de l'Ailaoshan-Fleuve Rouge, 148 pp., Ph.D. thesis, Univ. Pierre et Marie Curie (Paris 6), 1991.

Leloup, P.H., Y. Ricard, J. Battaglia, and R. Lacassin, Shear heating in continental strike-slip shear zones: Model and field examples, *Geophys. J. Int., 136*, 19-40, 1999.

Li, S.G., et al., Collision of the North China and Yangtze blocks and the formation of coesite-bearing eclogites: Timing and processes, *Chem. Geol., 109*, 89-111, 1993.

Li, Z.X., Collision between the north and south China blocks: A crust-detachment model for suturing in the region east of the Tan-Lu fault, *Geology, 22*, 739-742, 1994.

Lin, J.L., The apparent polar wander paths for the north and south China blocks, 248 pp., Ph.D. thesis, Univ. of Calif., Santa Barbara, 1984.

Liu, D.Y., Q.H. Shen, Z.Q. Zhang, B.M. Jahn, and B. Auvray, Archean crustal evolution in China: U-Pb geochronology of the Qianxi complex, *Precambrian Res., 48*, 223-244, 1990.

Liu, D.Y., A.P. Nutman, W. Compston, J.S. Wu, and Q.H. Shen, Remnants of > or =3800 Ma crust in the Chinese part of the Sino-Korean Craton, *Geology, 20*, 339-342, 1992.

Liu, M.W., H.Y. Luan, P.X. Chi, and L.J. Xu, On the division and correlation of the Jurassic-Cretaceous lithostratigraphy in Shandong Province, *Geol. Shandong*, 10 suppl., 53-68, 1994.

Mattauer, M., P. Matte, H. Maluski, Z.Q. Qin, Q.W. Zhang, and Y.M. Yong, Paleozoic and Triassic plate boundary between North and South China. New structural and radiometric data on the Dabie-Shan (eastern China), *C. R. Acad. Sci., Ser II, 312*, 1227-1233, 1991.

McElhinny, M.W., Statistical significance of the fold test in paleomagnetism, *Geophys. J. R. Astron. Soc., 8*, 338-340, 1964.

McFadden, P.L., and A.B. Reid, Analysis of palaeomagnetic inclination data, *Geophys. J. R. Astron. Soc., 69*, 307-319, 1982.

McFadden, P.L., and M.W. McElhinny, The combined analysis of remagnetization great circles and direct observations in paleomagnetism, *Earth Planet. Sci. Lett., 87*, 161-172, 1988.

McFadden, P.L., and M.W. McElhinny, Classification of the reversal test in palaeomagnetism, *Geophys. J. Int., 130*, 725-729, 1990.

Meyer, B., P. Tapponnier, L. Bourjot, F. Métivier, Y. Gaudemer, G. Peltzer, S.M. Guo, and Z.T. Chen, Crustal thickening in Gansu-Qinghai, lithospheric mantle subduction, and oblique, strike-slip growth of the Tibetan plateau, *Geophys. J. Int., 135*, 1-47, 1998.

Morton, W.H., and R. Black, Crustal attenuation in Afar, in *Afar Depression of Ethiopia*, edited by A. Pilger and A. Rösler, Inter. Union Comm. on Geodyn. Sci. Rep. no. 14, pp. 55-65, E. Schweizerbart'sche Verlagsbuch., Stuttgart, Germany, 1975.

Okay, A.I., A.M.C. Sengör, and M. Satir, Tectonics of an ultrahigh-pressure metamorphic terrane: The Dabie Shan/Tongbai Shan orogen, China, *Tectonics, 12*, 1320-1334, 1993.

Opdyke, N.D., K.N. Huang, G. Xu, and W.Y. Zhang, Paleomagnetic results from the Triassic of the Yangtze platform, *J. Geophys. Res., 91*, 9553-9568, 1986.

Peltzer, G., P. Tapponnier, Z.T. Zhang, and X.Z. Qin, Neogene and Quaternary faulting in and along the Qinling Shan, *Nature, 317*, 500-505, 1985.

Peltzer, G., and F. Saucier, Present-day kinematics of Asia derived from geologic fault rates, *J. Geophys. Res., 101*, 27943-27956, 1996.

Reischmann, T., U. Altenberger, A. Kröner, G. Zhang, Y. Sun, and Z. Yu, Mechanism and time of deformation and metamorphism of mylonitic orthogneisses from the Shagou Shear Zone, Qinling Belt, China, *Tectonophysics, 185*, 91-109, 1990.

Schmidt, P.W., Bias in converging great circle methods, *Earth Planet. Sci. Lett.*, *72*, 427-432, 1985.

Shandong Bureau of Geology and Mineral Resources (SDBGMR), *Regional Geology of Shandong Province*, 639 pp., Geol. Publ., Beijing, 1991.

Tapponnier, P., and P. Molnar, Active faulting and tectonics in China, *J. Geophys. Res.*, *82*, 2905-2930, 1977.

Tapponnier, P., Peltzer, G., A.Y. LeDain, and R. Armijo, Propagating extrusion tectonics in Asia: New insights from simple experiments with placticine, *Geology*, *10*, 611-616, 1982.

Tapponnier, P., G. Peltzer, and R. Armijo, On the mechanics of the collision between India and Asia, in *Collision Tectonics*, edited by M.P. Coward and A.C. Ries, *Geol. Soc. London Spec. Publ.*, *19*, 115-157, 1986.

Thompson, A.B., and J.A.D. Connolly, Melting of the continental crust: Some thermal and petrological constraints on anatexis in continental collision zones and other tectonic settings, *J. Geophys. Res.*, *100*, 15565-15579, 1995.

Uchimura, H., M. Kono, H. Tsunakawa, G. Kimura, Q. Wei, T. Hao, and H. Liu, Paleomagnetism of late Mesozoic rocks from northeastern China: The role of the Tan-Lu fault in the North China Block, *Tectonophysics*, *262*, 301-319, 1996.

Wageman, J.M., T.W.C. Hilde and K.O. Emery, Structural framework of East China Sea and Yellow Sea, *Am. Assoc. Petrol. Geol. Bull.*, *54*, 1611-1643, 1970.

Wang, X.M., J.G. Liou, and H.K. Mao, Coesite-bearing eclogite from Dabie Mountains in central China, *Geology*, *17*, 1085-1088, 1989.

Wang, Z., and R. Van der Voo, Pervasive remagnetization of Paleozoic rocks acquired at the time of Mesozoic folding in the South China Block, *J. Geophys. Res.*, *98*, 1729-1741, 1993.

Watson, G.S., and R.J. Enkin, The fold test in paleomagnetism as a parameter estimation problem, *Geophys. Res. Lett.*, *20*, 2135-2137, 1993.

Wei, S.Y., and J.W. Teng, Lithospheric structure and geophysical field, Tancheng-Lujiang fault zone, eastern China, in *The Tancheng-Lujiang Wrench Fault System*, edited by J.W. Xu, pp. 149-165, John Wiley, New York, 1993.

Xu, J.W., G. Zhu, W.X. Tong, K.R. Cui, and Q. Liu, Formation and evolution of the Tancheng-Lujiang wrench fault system: A major shear system to the northwest of the Pacific Ocean, *Tectonophysics*, *134*, 273-310, 1987.

Xu, J.W., Basic characteristics and tectonic evolution of the Tancheng-Lujiang fault zone, in *The Tancheng-Lujiang Wrench Fault System*, edited by J.W. Xu, pp. 17-50, John Wiley, New York, 1993.

Xu, S.T., L.L. Jiang, Y.C. Liu, and Z. Yong, Tectonic framework and evolution of the Dabie Mountains in Anhui, eastern China, *Acta Geol. Sin.*, *5*, 221-238, 1992a.

Xu, S.T., A.I. Okay, S.Y. Ji, A.M.C. Sengör, S. Wen, Y.C. Liu, and L.L. Jiang, Diamond from the Dabie Shan metamorphic rocks and its implication for tectonic setting, *Science*, *256*, 80-82, 1992b.

Xue, F., D.B. Rowley, and J. Baker, Refolded syn-ultrahigh-pressure thrust sheets in the south Dabie complex, China: Field evidence and tectonic implications, *Geology*, *24*, 455-458, 1996.

Xue, F., D.B. Rowley, R.D. Tucker, and Z.X. Peng, U-Pb Zircon ages of granitoid rocks in the North Dabie Complex, eastern Dabie Shan, China, *J. Geol.*, *105*, 744-753, 1997.

Yanai, S.C., S. Otoh, S. Yamakita, Y.J. Jwa, and B.S. Park, Honam intra-arc transcurrent fault and Jurassic Geodynamics in east Asia, in *The Tancheng-Lujiang Wrench Fault System*, edited by J.W. Xu, pp. 213-224, John Wiley, New York, 1993.

Ye, H., K.M. Shedlock, S.J. Hellinger, and J.G. Sclater, The North China Basin: An example of a Cenozoic rifted intraplate basin, *Tectonics*, *4*, 153-169, 1985.

Yin, A., and S.Y. Nie, An indentation model for the north and south China collision and the development of the Tan-Lu and Honam fault systems, eastern Asia, *Tectonics*, *12*, 801-813, 1993.

Yui, T.F., D. Rumble III, and C.H. Lo, Unusually low $\partial^{18}O$ ultra-high-pressure metamorphic rocks from the Sulu Terrain, eastern China, *Geochim. Cosmochim. Acta*, *13*, 2859-2864, 1995.

Yui, T.F., D. Rumble III, C.H. Chen, and C.H. Lo, Stable isotope characteristics of eclogites from the ultra-high-pressure metamorphic terrain, east-central China, *Chem. Geol.*, *137*, 135-147, 1997.

Zhang, R.Y., D. Rumble III, J.G. Liou, and Q.C. Wang, Low $\partial^{18}O$, ultrahigh-P garnet-bearing mafic and ultramafic rocks from Dabie Shan, China, *Chem. Geol.*, *150*, 161-170, 1998.

Zhang, S.F., Z.Q. Zhang, Z.Y. Song, and M.X. Gao, Stratigraphic division and correlation of the Carboniferous, Permian and Triassic strata in Shandong Province, *Geol. Shandong*, 10 suppl., 46-52, 1994.

Zhang, Y.Q., P. Vergely, and J. Mercier, Active faulting in and along the Qinling Range (China) inferred from SPOT imagery analysis and extrusion tectonics of south China, *Tectonophysics*, *243*, 69-95, 1995.

Zhang, Z.M., J.G. Liou, and R.G. Coleman, An outline of the plate tectonics of China, *Geol. Soc. Am. Bull.*, *95*, 295-312, 1984.

Zhao, X.X., A paleomagnetic study of Phanerozoic rock units from eastern China, Ph.D. thesis, 402 pp., Univ. of Calif. Santa Cruz, 1987.

Zhao, X.X., and R.S. Coe, Paleomagnetic constraints on the collision and rotation of north and south China, *Nature*, *327*, 141-144, 1987.

Zhao, X.X., and R.S. Coe, Tectonic implications of Permo-Triassic paleomagnetic results from north and south China, in *Deep Structure and Past Kinematics of Accreted Terranes*, *Geophys. Monogr. Ser.*, vol. 50, edited by J.W. Hillhouse, pp. 267-283, AGU, Washington, D. C., 1989.

Zhu, G., Xu, J.W., and S.Q. Sun, Isotopic age evidence for the timing of strike-slip movement of the Tan-Lu fault zone, *Geol. Rev.*, *41*, 452-456, 1995.

Zhu, Z.W., Late Mesozoic paleomagnetism in eastern China and the horizontal displacement of the Tancheng-Lujiang fault zone, in *The Tancheng-Lujiang Wrench Fault System*, edited by J.W. Xu, pp. 139-147, John Wiley, New York, 1993.

Zijderveld, J.D.A., A.C. demagnetization of rocks-analysis of results, in *Methods in Paleomagnetism*, edited by D.W. Collinson, K.M. Creer, and S.K. Runcorn, pp. 254-286, Elsevier, New York, 1967.

Y. Chen, Département des Sciences de la Terre, Université d'Orléans, B.P. 6759, 45067 Orléans, Cedex 02 France.

R. Coe and X. Zhao, Earth Science Department, University of California, Santa Cruz, CA 95064.

J-P. Cogné, V. Courtillot, S. Gilder, N. Halim, Institut de Physique du Globe, Laboratoire de Paléomagnétisme et Géodynamique, 4 Place Jussieu, 75252 Paris Cedex 05 France. (e-mail: gilder@ipgp.jussieu.fr).

P. Leloup, Institut de Physique du Globe de Paris, Laboratoire de Tectonique, 4 place Jussieu, 75252 Paris, Cedex 05 France.

W. Xiao, Laboratory of Lithosphere Tectonic Evolution, Institute of Geology, Chinese Academy of Sciences, P.O. Box 9825, Beijing 100029 China.

R. Zhu, Institute of Geophysics, Chinese Academy of Sciences, P.O. Box 9701, Beijing 100101 China.

(Received June 25, 1998; revised February 15, 1999;
accepted March 25, 1999.)